



HAL
open science

Climate change and the potential distribution of *Xylella fastidiosa* in Europe

Martin Godefroid, Astrid Cruaud, Jean-Claude Streito, Jean Yves Rasplus,
Jean-Pierre Rossi

► **To cite this version:**

Martin Godefroid, Astrid Cruaud, Jean-Claude Streito, Jean Yves Rasplus, Jean-Pierre Rossi. Climate change and the potential distribution of *Xylella fastidiosa* in Europe. 2018. hal-02791548

HAL Id: hal-02791548

<https://hal.inrae.fr/hal-02791548>

Preprint submitted on 5 Jun 2020

HAL is a multi-disciplinary open access archive for the deposit and dissemination of scientific research documents, whether they are published or not. The documents may come from teaching and research institutions in France or abroad, or from public or private research centers.

L'archive ouverte pluridisciplinaire **HAL**, est destinée au dépôt et à la diffusion de documents scientifiques de niveau recherche, publiés ou non, émanant des établissements d'enseignement et de recherche français ou étrangers, des laboratoires publics ou privés.



Distributed under a Creative Commons Attribution - NonCommercial 4.0 International License

1 **Climate change and the potential distribution of *Xylella fastidiosa* in Europe**

2
3 Martin Godefroid^{1,2}, Astrid Cruaud¹, Jean-Claude Streito¹, Jean-Yves Rasplus¹ and Jean-
4 Pierre Rossi^{1*}

5
6 ¹CBGP, INRA, CIRAD, IRD, Montpellier SupAgro, Univ. Montpellier Montpellier, France.

7 ²Present address: Fisheries & Oceans Canada, Pacific Biological Station, Nanaimo, B.C

8 *corresponding author: jean-pierre.rossi@inra.fr

9 10 **Abstract**

11 The bacterium *Xylella fastidiosa* (*Xf*) is a plant endophyte native to the Americas that
12 causes worldwide concern. *Xf* has been recently detected in several regions outside its
13 natural range including Europe. In that context, accurate estimates of its response to
14 climate change are required to design cost-efficient and environment-friendly control
15 strategies. In the present study, we collected data documenting the native and invaded
16 ranges of the three main subspecies of *Xf*: *fastidiosa*, *pauca* and *multiplex*, as well as two
17 strains of *Xf* subsp. *multiplex* recently detected in southern France (ST6 and ST7). We
18 fitted bioclimatic species distribution models (SDMs) to forecast their potential
19 geographic range and impact in Europe under current and future climate conditions.
20 According to model predictions, the geographical range of *Xf* as presently reported in
21 Europe is small compared to the large extent of suitable areas. The European regions
22 most threatened by *Xf* encompass the Mediterranean coastal areas of Spain, Greece, Italy
23 and France, the Atlantic coastal areas of France, Portugal and Spain as well as the south-
24 western regions of Spain and lowlands in southern Italy. Potential distribution of the
25 different subspecies / strains are contrasted but all are predicted to increase by 2050,
26 which could threaten several of the most economically important wine-, olive- and fruit-
27 producing regions of Europe, warranting the design of control strategies. Bioclimatic
28 models also predict that the subspecies *multiplex* might represent a threat to most of
29 Europe under current and future climate conditions. These results may serve as a basis
30 for future design of a spatially informed European-scale integrated management
31 strategy, including early detection surveys in plants and insect vectors, quarantine
32 measures as well as agricultural practices.

33
34 **Keywords** Pierce's disease, species distribution models, global change, biological
35 invasions, risk assessment

36 37 **Introduction**

38 The bacterium *Xylella fastidiosa* (*Xf*) is a plant endophyte native to the Americas, that
39 develops in up to 300 plant species including ornamental and agricultural plants ¹. In its
40 native range, *Xf* is transmitted between plants by xylem-feeding insects belonging to
41 several families of Hemiptera (Aphrophoridae, Cercopidae, Cicadellidae, Cicadidae and
42 Clastopteridae) ². *Xf* causes severe plant pathologies leading to huge economic losses ³,
43 including the Pierce's disease of grapevines PD: ⁴, the olive quick decline ⁵, the oak
44 bacterial leaf scorch ⁶, the phony peach disease ⁷, the *Citrus* variegated chlorosis CVC: ⁸
45 and the almond leaf scorch ⁹. As *Xf* can colonize a large number of economically
46 important plants including vine ¹, its biology and the mechanisms of vector transmission
47 have been extensively studied to design management strategies ¹⁰. On the basis of
48 genetic data obtained with Multilocus Sequence Typing MLST: ^{11,12}, *Xf* was subdivided
49 into six subspecies (*fastidiosa*, *pauca*, *multiplex*, *sandyi*, *tashke* and *morus*). The

50 subspecies were further characterized by different geographic origins, distributions and
51 host preferences in the Americas¹³⁻¹⁵. However, the status of the different subspecies is
52 still a matter of debate¹⁶ and only two, *fastidiosa* and *multiplex*, are formally considered
53 valid names^{1,17}. *Xf* subsp. *fastidiosa*¹⁸ occurs in North and Central America, where it
54 causes, among others, the harmful PD and the almond leaf scorch (ALS). Genetic
55 analyses suggest that this subspecies originated from southern parts of Central America
56¹⁹. The subspecies *multiplex* is widely distributed in North America (from California to
57 western Canada and from Florida to eastern Canada), where it was detected on a wide
58 range of host plants (e.g. oak, elm, maple, almond, sycamore, *Prunus* sp., etc.) as well as
59 in South America^{20,21}. The subspecies *pauca*, which causes severe diseases in *Citrus*
60 (CVC) and coffee (Coffee Leaf Scorch: ²²) in South and Central America, is thought to be
61 native to South America²³. The subspecies *morus* recently proposed by Nunney et al²⁴,
62 occurs in California and eastern USA, where it is associated to mulberry leaf scorch. *Xf*
63 subsp. *sandyi*, responsible for oleander leaf scorch, is distributed in California¹², while
64 the subspecies *tashke* was proposed by Randall et al²⁵ for a strain occurring on *Chitalpa*
65 *tashkentensis* in New Mexico and Arizona. Overall, intraspecific entities of *Xf* display
66 differences in host range suggesting that the radiation of *Xf* into multiple subspecies and
67 strains is primarily associated to host specialization²⁶.
68 *Xylella fastidiosa* is now of worldwide concern as human-mediated dispersal of
69 contaminated plant material has allowed the bacterium to spread outside its native
70 range. In 2013, the CoDIRO strain (subsp. *pauca*) was detected on olive trees in southern
71 part of the Apulia territory (Italy). Genetic analyses suggested that it was accidentally
72 introduced from Costa Rica or Honduras with infected ornamental coffee plants⁵. Since
73 then, *Xf* subsp. *pauca* has spread northward and killed millions of olive trees in the
74 Apulia territory, causing unprecedented socio-economic issues. During the period 2015-
75 2017 several subspecies and strains were detected on *ca* 30 different host plants in
76 Southern France (PACA region) and Corsica²⁷. According to this survey, the vast
77 majority of plant samples were contaminated by two strains of *Xf* subsp. *multiplex*
78 (referred here to as the French ST6 and ST7 strains). These strains are closely related to
79 the Californian strains Dixon (ST6) and Griffin (ST7), belonging to the “almond group” of
80 Nunney et al (2013) and were detected on numerous plant species though without
81 evident specialization. To a lesser extent, other strains were detected in Southern
82 France. Thus, the strain ST53 (*Xf* subsp. *pauca*) was detected on *Polygala myrtifolia* in
83 Côte d’Azur (Menton) and on *Quercus ilex* in Corsica²⁷. Finally, recombinants strains
84 (ST76, ST79 or not yet fully characterized) were detected in a few plant samples. In
85 2016, *Xf* subsp. *fastidiosa* was detected on rosemary and oleander plants overwintering
86 in a nursery in Germany²⁸. In 2017, Spanish plant biosecurity agencies officially
87 confirmed the detection of *Xf* strains belonging to the subspecies *multiplex*, *pauca* and
88 *fastidiosa* on almond trees, grapevine, cherry and plums in western parts of the Iberian
89 Peninsula and Balearic islands²⁹. Outside Europe, the detection of *Xf* was officially
90 confirmed in Iran on almond trees and grapevines³⁰, in Turkey³¹ as well as in Taiwan
91 on grapevines³². The severity of *Xf*-induced diseases has recently dramatically increased
92 in several areas possibly due to global warming³³. Indeed, it has been demonstrated
93 that cold winter temperatures might affect the survival of *Xf* in xylem vessels and allow
94 plants to partly recover from *Xf*-induced diseases ‘cold curing phenomenon’:^{34,35}. For
95 instance, Purcell³⁴ showed that grapevines with symptoms of PD recovered after
96 multiple exposures to temperatures below -8°C during several hours. Further, Anas et al
97³⁶ suggested that areas experiencing more than 2 to 3 days with minimal temperature
98 below -12.2 °C (or alternatively 4 to 5 days below -9.9 °C) should be considered at low

99 risk for PD incidence, although these thresholds were considered too conservative by
100 Lieth et al ³⁷. There is no doubt that estimating the potential distribution of *Xf* under
101 current and future climate conditions will contribute to design environment-friendly
102 and cost-efficient management strategies ³⁸. Several studies aimed to forecast the
103 potential distribution of *Xf* in Europe ³⁹ and/or all over the world ⁴⁰. For instance,
104 Hoddle et al ⁴⁰ used the CLIMEX algorithm to forecast the worldwide potential severity
105 of PD without accounting for potential future range shifts induced by global change.
106 Bosso et al ³⁹ fitted a Maxent model to forecast the potential distribution of *Xf* subsp.
107 *pauca* under current and future climate conditions, and concluded that climate change
108 would not affect its future distribution of *Xf*. However, Bosso et al ³⁹ calibrated their
109 model using solely the presence records from the invaded range in Italy, a practice that
110 is known to increase omission errors ⁴¹.
111 Here, to assist in designing efficient survey as well as appropriate management
112 strategies of *Xf* in Europe, we modeled the potential distribution of three of its
113 subspecies: *fastidiosa*, *pauca* and *multiplex* under current and future climate conditions.
114 For finest estimates we also modeled the potential distribution of the two strains of the
115 subsp. *multiplex* that seem largely distributed in Southern France (i.e. the French ST6
116 and ST7). Finally, to go one step further, we estimated the severity of the Pierce's
117 Disease (caused by *Xf* subsp. *fastidiosa*) in European ecosystems based on US Pierce
118 Disease intensity/occurrence maps provided by A. Purcell (available in Kamas et al ⁴²
119 and in Anas et al ³⁶).

120

121 **Material & Methods**

122

123 *Distribution data*

124

125 We collected occurrence data for subspecies *pauca* and *multiplex* in both their native
126 and invaded ranges from the scientific literature, field surveys and public databases (Fig.
127 1). We also used data on the distribution of the strains ST6 and ST7 in France that were
128 collected in 2015-2017 and stored in the French national database managed by the
129 French Agency for Food, Environmental and Occupational Health & Safety (ANSES) (Fig.
130 1B). For the subspecies *fastidiosa*, we randomly generated 400 occurrences within its
131 traditional range and assigned to each record a PD severity index (index 1: low severity;
132 index 2: moderate severity; index 3: high severity) according to PD intensity maps
133 provided by A. Purcell (available in Anas et al ³⁶ and Kamas et al ⁴²) (Fig. 1A). High
134 severity regions comprise Florida, south of Alabama, Texas, Louisiana and Mississippi
135 states as well as Los Angeles basin in California and coastal areas of South and North
136 Carolina (Fig. 1A). Moderate severity areas comprise north of Alabama, Georgia, Texas,
137 Louisiana and Mississippi states as well as some wine-producing regions of California
138 (Napa valley, Sonoma valley, Santa Clara valley) where severe PD outbreaks occurred
139 during the 20th century even though it was an unusual phenomenon. Low severity
140 regions encompass most of Virginia, Oklahoma, North Texas, Kentucky etc. as well as
141 localities in Washington State ³⁴. Pierce's disease symptoms associated to the presence
142 of *Xf* were recently detected in West Virginia ³³, Oklahoma ⁴³ and high elevation regions
143 of Texas ⁴². The emergence of PD in these regions may, however, have been induced by
144 the recent increase of temperatures occurring in the late 1990's and in 2000's. We
145 deliberately considered these regions as low-risk areas because climate descriptors
146 used in the present study represent average climate conditions for the 1970-2000

147 period (see below) and do not account for temperature changes that occurred at the
148 very end of the 20th century and the beginning of the 21th century.

149

150 *Bioclimatic descriptors*

151

152 We used a set of bioclimatic descriptors hosted in the Worldclim database bio1 to bio19
153 see ⁴⁴. We used raster layers of 2.5-minute spatial resolution, which corresponds to
154 about 4.5 km at the equator. The data come in the form of a raster map and represent
155 the average climate conditions for the period 1970-2000. We estimated the future
156 potential distributions of the different subspecies of *Xf* in 2050 and 2070 using the
157 Model for Interdisciplinary Research on Climate version 5 MIROC5 ⁴⁵. These predictions
158 of future temperature and precipitation rank among the most reliable according to
159 model evaluation procedures used in AR5 of IPCC ⁴⁶. We used two different climatic
160 datasets relative to the representative concentration pathways RCP4.5 and RCP8.5,
161 which assume moderate and extreme global warming, respectively ⁴⁷.

162

163 *Models*

164

165 The PD severity index being an ordinal categorical variable (1<2<3) it was modeled
166 using a cumulative link model (CLM) also called ordinal regression models, or
167 proportional odds models ⁴⁸. The CLM analyses the relationship between a set of
168 independent variables (the climate descriptors) and an ordinal dependent variable
169 consisting in the PD severity index. The CLM was fitted using a dataset corresponding to
170 Pierce's disease intensity in the US (Fig. 1A). It was then used to compute the spatial
171 distribution of the probabilities that the different classes of index occur in Europe. CLM
172 fit and predictions were carried out using the R software version 3.3.3 ⁴⁹ and the R
173 packages MASS ⁵⁰ and ordinal ⁵¹.

174 The potential distribution of *Xf* subsp. *pauca*, *multiplex* and the French ST6/ST7 were
175 estimated using species distribution modeling. Species distribution models establish
176 mathematical species-environment relationships using presence records and
177 environmental descriptors in order to assess the potential distribution of species or map
178 the habitat suitability ⁵². We used two presence-only approaches namely Bioclim ^{53,54}
179 and Domain ⁵⁵. These algorithms are climatic envelope approaches. As such, they are
180 based on presence records and do not make any assumptions about the absence of the
181 organism under study. We selected these approaches because they are well suited to
182 poorly documented species for which reliable absences are unavailable ^{54,56}. In addition,
183 we deliberately did not fit SDMs which rely on complex mathematical relationships
184 among descriptors such as e.g. Maxent: ⁵⁷ as we used only a few climate descriptors (see
185 below).

186 Both Bioclim and Domain yield an index of habitat suitability that can be categorized to
187 form a binary map (species presence vs. absence or suitable vs. unsuitable habitat). We
188 used the lowest presence threshold (LPT) ⁵⁸ i.e. the lower value of predicted climatic
189 suitability associated to presence records. SDM fit and predictions were carried out
190 using the R package *dismo* ⁵⁹.

191

192

193

194

195

196 *Procedure to select climate predictors*

197

198 The models were intentionally fitted using a limited number of ecologically relevant
199 climate descriptors to avoid model over-parameterization, which is a recommended
200 practice in the context of invasion risk assessment ⁶⁰.

201 CLM. Although *Xf* geographical distribution appears to be primarily driven by minimum
202 temperatures, the dynamics of the plant-pathogen-vector system is complex ⁶¹ and
203 rainfall may impact the severity of the disease by affecting the bacterium pathogenicity
204 or the intensity of the vector by insects.

205 The CLM was fitted using a set of climate variables that represent possible significant
206 ecological stressors (maximum temperature of warmest month (bio5), minimum
207 temperature of coldest month (bio6), mean temperature of warmest quarter (bio10),
208 mean temperature of coldest quarter (bio11), precipitation of wettest quarter (bio16),
209 precipitation of driest quarter (bio17), precipitation of warmest quarter (bio18) and
210 precipitation of coldest quarter (bio19)). We used a stepwise model selection by AIC to
211 identify the best performing variable subset, which finally comprised (bio10: mean
212 temperature of warmest quarter, bio11: mean temperature of coldest quarter and
213 bio18: precipitation of warmest quarter). Because the impact of precipitations upon PD
214 severity pattern at large spatial scales is not well documented we performed the
215 computations using the full model (bio10, bio11 and bio18) and a model comprising
216 only the temperature predictors (bio10 and bio11).

217

218 SDM. A first step consisted into fitting and evaluating both Bioclim and Domain models
219 using 10 different climate datasets combining maximal and minimal temperatures
220 descriptors (bio5: maximum temperature of the warmest month; bio6: minimum
221 temperature of the coldest month; bio10: mean temperature of the warmest quarter;
222 bio11: mean temperature of the coldest quarter) (Table 1). We did not include
223 descriptors of rainfall since we were interested in modeling distribution only (not
224 severity) ³⁴. At this stage, models were fitted using only the occurrences available in the
225 native area of each subspecies or French occurrences of the ST6 and ST7 strains (Fig. 1B,
226 C, D). This allowed us to evaluate the transferability of each model by calculating the
227 proportion of actual presences in the invaded range correctly predicted using the LPT ⁵⁸
228 i.e. model sensitivity. As a second evaluation of model transferability, we calculated the
229 area under the curve of the receiver operator curve (AUC) from a dataset encompassing
230 occurrences available in Europe as well as 10,000 pseudo-absences randomly generated
231 across the European territory. For a given subspecies, the climatic dataset associated to
232 models showing poor transferability were discarded from the study. The selected
233 climate dataset were then used to fit Bioclim and Domain models using the occurrences
234 available in both native and invaded ranges as recommended by various authors e.g.
235 Broennimann and Guisan ⁴¹. The models were used to estimate the habitat suitability
236 across Europe and binary maps were generated using the threshold detailed above. For
237 each taxonomic unit we finally constructed a suitability map by averaging the
238 predictions of models fitted with each selected set of climatic descriptors ensemble
239 forecasting: ^{62,63}.

240

241 *Refining species distribution models' predictions*

242

243 Some points in Europe may be associated to climate conditions that are not encountered
244 within the range of conditions characterizing the set of reference points i.e. within the

245 native and invaded areas. In such situations, using the species distribution models to
246 predict habitat suitability in such novel habitats can be misleading ⁶⁴. Elith et al ⁶⁴
247 introduced the multivariate environmental similarity surface (MESS) to quantify how
248 similar a point is to a reference set of points with respect to a set of predictor variables.
249 Negative values of the MESS index indicate sites where at least one variable has a value
250 lying outside the range of environments over the reference set. We computed the MESS
251 index over Europe with reference to the occurrence dataset used to fit each species
252 distribution model. We further restricted the model predictions to areas where the
253 index was positive. We used a MESS index computed with the variable bio11 (mean
254 temperature of coldest quarter) to refine the CLM predictions because the impact of
255 winter temperatures on PD dynamics is very well documented ^{34,35,65}. MESS
256 computations were carried out using the R package `dismo` ⁵⁹. All graphical outputs were
257 produced using the R packages `ggplot2` ⁶⁶ and `cowplot` ⁶⁷.

258

259 **Results**

260

261 *Pierce's disease severity index*

262

263 The stepwise-selected model comprised three bioclimatic descriptors: bio10: mean
264 temperature of warmest quarter, bio11: mean temperature of coldest quarter and
265 bio18: precipitation of warmest quarter. The variable contribution was highly
266 significant in all cases ($p < 10^{-3}$) and the coefficients were -19.4 (bio10), 77.6 (bio11) and
267 3.5 (bio18). The resulting model was used to compute the values of the PD severity
268 index across North America and Europe using climatic dataset corresponding to the
269 period 1970-2000. In North America the MESS index revealed that areas north of 35
270 decimal degrees latitude were associated to strongly negative index (Fig. S1). In Europe,
271 low index values were observed in north-eastern areas as well as in the Alps and the
272 Pyrenees (Fig. S2). These areas were discarded from further interpretation and have
273 been subsequently depicted in grey in the maps shown in Fig. 2. The Figs 2A and S3
274 show the model predictions for the three levels of severity in Europe and North America
275 for the period 1970-2000 respectively.

276 The CLM predicted a risk of moderate to highly severe PD in multiple lowlands and
277 coastal areas of the Mediterranean regions (Spain, Italy, Balearic islands and North
278 Africa) as well as along the Atlantic coasts of France, Northern Spain and Portugal (Fig.
279 2A). A low to moderate severity of PD was also predicted in the Atlantic coasts of France,
280 lowlands of northern Italy, and central Spain. High severity was predicted in Sicilia
281 (Italy), and along both the Atlantic and Mediterranean coasts of Spain.

282 Using the model to estimate the PD severity index according to different climate change
283 scenarios led to the maps displayed in Fig. 2B and 2C for 2050 and Fig. S4 B and C for
284 2070. In each case, the MESS index was recomputed on the basis of the present and
285 future climate conditions. Estimations for 2050 indicate an increased PD severity in
286 south Italy, Corsica and Sardinia either with the concentration pathways RCP4.5 or the
287 RCP8.5 (Fig. 2B, and 2C). The estimates for 2070 are pretty much similar (Fig. S4).

288 The CLM fitted with only bio10 and bio11 led to the results showed in Fig. S5 and S6.
289 The main differences are that the Atlantic coasts of France, Ireland and west England are
290 associated to severity index of 1 whereas the model including bio18 predicted a severity
291 of 2 (Fig. S5). A similar pattern is observed for the predictions in 2070 (Figs S4 and S6).

292

293

294 *Potential distribution of Xf subspecies pauca and multiplex*

295

296 Both Bioclim and Domain fitted using climate datasets #1, #4 and #7 yielded high
297 transferability measures (AUC superior to 0.85 and sensitivity = 1) in the case of the
298 subsp. *pauca* (Table 1). These datasets were therefore retained for further analyses. For
299 the subsp. *multiplex* we selected 3 climate datasets (#2, #6 and #9) associated to AUC
300 values >0.85 and a sensibility of 0.999 (Table 1).

301 Regarding the subspecies *pauca*, the models showed that climatically suitable
302 environments in Europe only correspond to small well-delimited areas in South
303 Portugal and Spain, Balearic Islands, Sicilia and North Africa (Fig. 3A). There was a
304 marked agreement between the models that all indicated very favorable environment in
305 these areas (Fig. 3D). It is worth noting that the areas associated to negative MESS index
306 values are very large (shaded areas in maps; i.e. areas experiencing climate conditions
307 absent from the dataset used to calibrate the model and for which no prediction was
308 made). This conveys the fact the subsp. *pauca* originates from South America (Fig. 1D)
309 and is associated to tropical environments. Suitable environments in Europe are
310 restricted to warmest environments around the Mediterranean Sea. The models predict
311 changes in the location of suitable areas in Europe by 2050 (Fig. 3B-F). Areas at risk
312 would include northern coast of Spain, south France and Tyrrhenian coast of Italy. There
313 is no marked differences according to the scenario examined (Fig. 3) and a similar
314 pattern is expected in 2070 (Fig. S7) except for Italy where climate conditions may
315 become unfavorable according to scenario 8.5 (Fig S7F).

316 The situation is different for the subspecies *multiplex* which is natively distributed
317 across North America (Fig. 1C) and for which the models depicted suitable conditions in
318 most of Europe except high-elevation areas and cold northern regions (Fig. 4). The
319 expected impacts of climate change are limited and mostly concern South Spain where
320 the conditions are expected to become unfavorable by 2050 and North part of Europe
321 that are predicted to become more favorable by 2050 (Fig. 4 B to F) and 2070 (Fig. S8).

322 The potential distribution of the French strains ST6 and ST7 is localized to
323 Mediterranean areas (Corsica, Sardinia, Sicilia and coastal areas of Italy and France)
324 (Fig. 5A, D). Suitable conditions are also present in the Atlantic coasts of Portugal and in
325 South West France. A shift in distribution is expected to occur by 2050 (Fig. 5B to F and
326 Fig. S9). Favorable conditions are expected to extend northward while areas currently
327 suitable such as South Western France are expected to become unfavorable. All models
328 indicate that the Spanish Atlantic coast (Galicia, Asturias, Cantabria and Basque country)
329 is expected to become climatically suitable by 2050.

330

331 **Discussion**

332

333 *Geographical distribution and possible impacts in Europe*

334

335 In a rapidly changing world, the design of pest control strategies (e.g. early detection
336 surveys and planning of phytosanitary measures) should ideally rely on accurate
337 estimates of the potential distribution and/or impact of pest species as well as their
338 responses to climate change³⁸. In the present study, bioclimatic models predicted that a
339 large part of the Mediterranean lowlands and Atlantic coastal areas are seriously
340 threatened by *Xf* subsp. *fastidiosa*, *multiplex* and *pauca*. A low to moderate impact is also
341 expected in northern and eastern regions of Europe (North-eastern France, Belgium, the
342 Netherlands, Germany, Scandinavia, the Baltic region, Poland, Austria, Switzerland, etc.)

343 that experience lower minimal temperature in winter but may nevertheless presumably
344 host *Xf* subsp. *multiplex*.

345 Models display good evaluation measures and predict moderate to high climatic
346 suitability in all European areas where symptomatic plants are currently infected by the
347 subspecies *fastidiosa*, *pauca* or *multiplex* (e.g. Balearic Islands, lowlands of Corsica
348 island, south-eastern France and the Apulia region). This suggests that risk maps
349 provided in the present study are reliable for the design of surveys, including ‘spy
350 insects’ survey^{68,69}. They may also be helpful to anticipate the spread of the different
351 subspecies and provide guidance on which areas should be targeted for an analysis of
352 local communities of potential vectors and host plants to design management strategies
353 and research projects.

354 Our results show that the subspecies/strains of *Xf* studied here might significantly
355 expand in the near future, irrespective of climate change. For example, the ST6 and ST7
356 strains (subsp. *multiplex*) present in Corsica and southern France have a large potential
357 for expansion, whose dynamics actually depends more on plant exchanges and disease
358 management than on climate suitability *per se*. The subspecies *multiplex* is associated to
359 economically important plants such as almonds and olives²⁶ but may also colonize
360 multiple ornamental plants. Its present potential distribution in Europe extends far
361 beyond areas where the subspecies has been reported and comprises Portugal, Italy,
362 and both South and South-western France suggesting possible important economical
363 losses.

364 The subspecies *fastidiosa*, which has been currently reported from a limited number of
365 localities, could encounter favorable climate conditions in various areas of Europe. The
366 model estimation of areas with a risk of PD highlights strategic wine-growing areas in
367 different countries. Notably, the present estimates of the potential impact of the subsp.
368 *fastidiosa* are consistent with the risk maps provided by Hoddle et al⁴⁰ and A. Purcell
369 (available in Anas et al³⁶). The case of subsp. *pauca* is somewhat different. Most of the
370 European occurrences are known from southern Italy and the Balearic Islands and the
371 potential distribution of this subspecies appears to be limited. This is not surprising
372 given that *Xf* subsp. *pauca* is native from South America and occupies a climatic niche
373 that mostly corresponds to areas located around the Mediterranean basin. Nevertheless,
374 southern Spain, Portugal, Sicilia and North Africa that are areas where growing olive
375 trees is multiseccular offer suitable conditions, which potentially implies huge socio-
376 economic impacts. One factor that proved to be critical for some diseases is the
377 distribution/availability of vectors and hosts. Here, none of these factors is limiting since
378 *Xf* is capable of colonizing a vast array of plants present in Europe and *Philaenus*
379 *spumarius*, the only European vector identified so far^{70,71}, occurs across the whole
380 continent⁶⁹.

381 Because we used the MESS index to discard regions experiencing climate conditions
382 absent from the dataset used to calibrate the model, our estimations of potential
383 distributions are conservative. The CLM showed a positive effect of higher temperatures
384 during the coldest quarter (variable bio11 associated to a positive coefficient) on the
385 severity index which may indicate to a lower “cold curing” effect^{34,65}. Absence of
386 estimation of the potential distribution of *Xf* (all subspecies) or of the PD severity index
387 (*Xf* subsp. *fastidiosa*) (i.e. shaded areas of the maps) does not mean that the bacterium is
388 unable to develop but rather that evaluating the risk is difficult. For example, the
389 potential impact of *Xf* in areas experiencing extremely high temperatures in summer
390 (e.g. southern and central Spain) remains largely uncertain as the impact of extreme
391 heat on *Xf* and on the behavior of insect vectors is still poorly known⁶¹. We report a

392 negative coefficient for the variable bio10 (mean temperature of the warmest quarter)
393 suggesting that PD severity would be negatively related to high temperatures during
394 summer. Although warm spring and summer temperatures enhance multiplication of *Xf*
395 in plants, it has been showed that *Xf* populations decrease in grapevines exposed to
396 temperatures above 37°C³⁵. As southern and central Spain frequently experience
397 temperatures above 40°C in summer, further field and laboratory experiments are
398 required to improve our estimation of the potential impact of *Xf* in these regions.
399 Another point requiring clarification is the effect of precipitation during the warmest
400 quarter that appears to be significant in the CLM. Precipitation may have direct impacts
401 on the dynamics of the relationship between *Xf* and its host as well as indirect effects
402 through the relationships with the insect vectors.

403

404 *Climate change and possible range shifts*

405

406 Our results clearly indicate that climate change may strongly impact the distribution of
407 *Xf* in Europe. Indeed, as “cold curing” appears to be the main mechanism explaining the
408 lower impact of *Xf* in colder regions, an increase of winter temperatures should make
409 these regions more suitable for *Xf* in the next decades^{34,35,65}. We report possible
410 changes in the potential distribution of the subspecies *multiplex* with a northward
411 expansion by 2070. The potential distribution of the French strains ST6 and ST7 is even
412 more impacted with a gradual shift of suitable areas from Southern France, Italy and
413 Portugal towards Northern France, Belgium, Netherlands and South England. The
414 suitable areas for *Xf* subsp. *pauca* are expected to slightly extend to the Mediterranean
415 coastal areas of Spain and France. The expected impact of climate change on the severity
416 index of the PD is less marked and mostly correspond to an increased PD severity in
417 south Italy, Corsica and Sardinia.

418 Overall, these results obtained on the different subspecies clearly indicate that climate
419 change will alter areas at risk for invasion by *Xf* in Europe. Given that both the
420 concentration pathways RCP4.5 and RCP8.5 led to concordant predictions, it appears
421 sound to expect such changes even if the global warming is kept to a moderate level.
422 SDMs showed that the subspecies *multiplex* displays a wider temperature tolerance and
423 could threaten most of the European continent now and in the future. This is not
424 surprising as this subspecies infects elms in regions of Canada characterized by low
425 winter temperatures⁷². This broad tolerance to cold is not known for other subspecies
426 and it is still unclear whether realized niche divergence among subspecies reflects
427 inherent differences in thermal tolerances or rather host-pathogen interactions as it was
428 observed for *Ralstonia solanacearum*⁷³. More investigations would help a better
429 understanding of the effect of temperatures on the different strains of *Xf*. It is
430 noteworthy that both present and future distributions show several areas of potential
431 co-occurrence. This may have important implications as it may increase the risk of
432 intersubspecific homologous recombination (IHR).

433

434 *Limits and opportunities for risk assessment*

435

436 Maps of habitat suitability and their declination with regards to future climate
437 conditions should be guardedly interpreted as they are derived from correlative tools
438 that depict the *realized* niche of species i.e. a subset of the *fundamental* environmental
439 tolerances constrained by biotic interactions and dispersal limits⁷⁴. In addition, we
440 cannot rule out the possibility that this study overestimates the potential distribution of

441 the subspecies *pauca* and *multiplex*, and of the French strains ST6 and ST7 under future
442 climate conditions. Indeed, time-periods associated to occurrences and climate
443 descriptors dataset do not perfectly overlap. The models were fitted with climate
444 descriptors that represent average climate conditions for the 1970-2000 period, while
445 most presence records were collected after 2000 in a period characterized by milder
446 winter temperatures. Moreover, as we deliberately fitted simple climate-envelope
447 approaches such as Bioclim and Domain based on few climate descriptors to avoid
448 model over-parameterization and/or extrapolation and enhance model transferability,
449 we cannot exclude that bioclimatic models presented in the study do not capture the
450 entire range of environmental tolerances and do not depict the complexity of the
451 climatic niche of *Xf* as well as potential interactions between climate descriptors. Better
452 models hence better risk assessment could be obtained if the amount of occurrence data
453 could be increased. True absences i.e. locations where the environmental conditions are
454 unsuitable for *Xf* to survive, would be particularly precious because they would allow
455 using powerful approaches such as the generalized linear model⁵². Finally, the possible
456 adaptation of the subspecies of *Xf* to environmental constraints met in European
457 ecosystems is another important and unknown factor of uncertainties. For example, the
458 potential of recombinant strains to adapt should be addressed in the near future.
459 Finally, it is worth noting that bioclimatic models predict climatic suitability of a
460 geographic region rather than a proper risk of *Xf*-induced disease incidence. To predict
461 the proper severity of *Xf*-induced diseases in a given locality, statistical models should
462 account for many additional factors playing a role in *Xf* epidemiology, including e.g.
463 microclimate conditions, inter-annual climate variability, landscape structure and the
464 spatio-temporal structure of the community of potential vectors. Although recent
465 entomological studies identified the meadow spittlebug *P. spumarius* as the main vector
466 of *Xf* in Italy^{70,71}, a better knowledge of all European vectors capable of transmitting *Xf*
467 from plant to plant as well as their ecological characteristics (geographic range,
468 efficiency in *Xf* transmission, demography, overwintering stage, etc.) is needed⁷⁵. In this
469 context, our estimates could allow to design cost-efficient vector surveys, with priority
470 given to geographic regions predicted as highly climatically suitable for *Xf*. The study by
471 Cruaud et al⁶⁹ provides a good insight into how species distribution modeling and DNA
472 sequencing approaches may be combined for an accurate monitoring of the range of *Xf*
473 and its vectors in Europe. We believe that bioclimatic models are promising tools to help
474 designing research experiments, control strategies as well as political decisions at the
475 European scale.

476

477 **Conclusions/highlights**

478

479 Species distribution models all indicate that the geographical range of *Xf* as presently
480 reported in Europe is small compared to the large extent of suitable areas. This is true
481 for all studied subspecies of *Xf* although the subspecies *pauca* appears to have a smaller
482 potential range possibly because of its Neotropical origin. Although caution is needed in
483 interpreting spatial projections because uncertainties in future climate conditions
484 themselves and because uncertainties associated to the predictions of the species
485 distribution models are difficult to assess, we showed that climate change will probably
486 affect the future distribution of the bacterium by 2050 and then 2070. Last but not least,
487 *Xf* has a certain potential to adapt for the specific climate and biotic interactions (hosts,
488 vectors) present in Europe. This potential is unknown but could nevertheless lead to
489 marked divergence between its future geographical distribution and the picture we have

490 of it today. However, our current knowledge allows proposing different research
491 avenues to better understand and anticipate the possible expansion of *Xf* in Europe.
492 European areas at risk encompass diversified (sub)natural ecosystems as well as agro-
493 ecosystems in which an important research effort should be made to decipher the host
494 plants – insect vectors – bacterium interactions⁷⁶. Only in this way could we develop an
495 appropriate and efficient strategy to deal with *Xf* in the coming years.

496
497

498 References

499

- 500 1 EFSA. Scientific Opinion on the risks to plant health posed by *Xylella fastidiosa* in
501 the EU territory, with the identification and evaluation of risk reduction options.
502 *EFSA Journal* **13**, 3989 (2015).
- 503 2 Janse, J. & Obradovic, A. *Xylella fastidiosa*: its biology, diagnosis, control and risks.
504 *Journal of Plant Pathology*, S35-S48 (2010).
- 505 3 Tumber, K., Alston, J. & Fuller, K. Pierce's disease costs California \$104 million per
506 year. *California Agriculture* **68**, 20-29 (2014).
- 507 4 Davis, M. J., Purcell, A. H. & Thomson, S. V. Pierce's disease of grapevines: isolation
508 of the causal bacterium. *Science* **199**, 75-77 (1978).
- 509 5 Martelli, G., Boscia, D., Porcelli, F. & Saponari, M. The olive quick decline
510 syndrome in south-east Italy: a threatening phytosanitary emergency. *European*
511 *Journal of Plant Pathology* **144**, 235-243 (2016).
- 512 6 Hearon, S. S., Sherald, J. L. & Kostka, S. J. Association of xylem-limited bacteria
513 with elm, sycamore, and oak leaf scorch. *Canadian Journal of Botany* **58**, 1986-
514 1993 (1980).
- 515 7 Wells, J. M., Raju, B. & Nyland, G. Isolation, culture and pathogenicity of the
516 bacterium causing phony disease of peach. *Phytopathology* **73**, 859-862 (1983).
- 517 8 Chang, C. J., Garnier, M., Zreik, L., Rossetti, V. & Bové, J. M. Culture and serological
518 detection of the xylem-limited bacterium causing citrus variegated chlorosis and
519 its identification as a strain of *Xylella fastidiosa*. *Current Microbiology* **27**, 137-142
520 (1993).
- 521 9 Davis, M., Thomson, S. & Purcell, A. Etiological role of a xylem-limited bacterium
522 causing Pierce's disease in almond leaf scorch. *Phytopathology* **70**, 5 (1980).
- 523 10 Almeida, R. P. & Nunney, L. How do plant diseases caused by *Xylella fastidiosa*
524 emerge? *Plant Disease* **99**, 1457-1467 (2015).
- 525 11 Scally, M., Schuenzel, E. L., Stouthamer, R. & Nunney, L. Multilocus sequence type
526 system for the plant pathogen *Xylella fastidiosa* and relative contributions of
527 recombination and point mutation to clonal diversity. *Applied and Environmental*
528 *Microbiology* **71**, 8491-8499 (2005).
- 529 12 Yuan, X. *et al.* Multilocus sequence typing of *Xylella fastidiosa* causing Pierce's
530 disease and oleander leaf scorch in the United States. *Phytopathology* **100**, 601-
531 611 (2010).
- 532 13 Nunney, L., Ortiz, B., Russell, S. A., Sánchez, R. R. & Stouthamer, R. The complex
533 biogeography of the plant pathogen *Xylella fastidiosa*: genetic evidence of
534 introductions and subspecific introgression in Central America. *PLoS One* **9**,
535 e112463 (2014).
- 536 14 Nunney, L., Elfekih, S. & Stouthamer, R. The importance of multilocus sequence
537 typing: cautionary tales from the bacterium *Xylella fastidiosa*. *Phytopathology*
538 **102**, 456-460 (2012).

- 539 15 Schuenzel, E. L., Scally, M., Stouthamer, R. & Nunney, L. A multigene phylogenetic
540 study of clonal diversity and divergence in North American strains of the plant
541 pathogen *Xylella fastidiosa*. *Applied and Environmental Microbiology* **71**, 3832-
542 3839 (2005).
- 543 16 Marcelletti, S. & Scortichini, M. Genome-wide comparison and taxonomic
544 relatedness of multiple *Xylella fastidiosa* strains reveal the occurrence of three
545 subspecies and a new *Xylella* species. *Archives of Microbiology* **198**, 803-812
546 (2016).
- 547 17 Bull, C. *et al.* List of new names of plant pathogenic bacteria (2008-2010). *Journal*
548 *of Plant Pathology* **94**, 21-27 (2012).
- 549 18 Wells, J. M. *et al.* *Xylella fastidiosa* gen. nov., sp. nov.: gram-negative, xylem-limited,
550 fastidious plant bacteria related to *Xanthomonas* spp. *International Journal of*
551 *Systematic and Evolutionary Microbiology* **37**, 136-143 (1987).
- 552 19 Nunney, L. *et al.* Population genomic analysis of a bacterial plant pathogen: novel
553 insight into the origin of Pierce's disease of grapevine in the US. *PLoS One* **5**,
554 e15488 (2010).
- 555 20 Nunes, L. R. *et al.* Microarray analyses of *Xylella fastidiosa* provide evidence of
556 coordinated transcription control of laterally transferred elements. *Genome*
557 *Research* **13**, 570-578 (2003).
- 558 21 Coletta-Filho, H. D., Francisco, C. S., Lopes, J. R., Muller, C. & Almeida, R. P.
559 Homologous recombination and *Xylella fastidiosa* host-pathogen associations in
560 South America. *Phytopathology* **107**, 305-312 (2017).
- 561 22 De Lima, J. *et al.* Coffee leaf scorch bacterium: axenic culture, pathogenicity, and
562 comparison with *Xylella fastidiosa* of citrus. *Plant Disease* **82**, 94-97 (1998).
- 563 23 Nunney, L., Yuan, X., Bromley, R. E. & Stouthamer, R. Detecting genetic
564 introgression: high levels of intersubspecific recombination found in *Xylella*
565 *fastidiosa* in Brazil. *Applied and Environmental Microbiology* **78**, 4702-4714
566 (2012).
- 567 24 Nunney, L., Schuenzel, E. L., Scally, M., Bromley, R. E. & Stouthamer, R. Large-scale
568 intersubspecific recombination in the plant-pathogenic bacterium *Xylella*
569 *fastidiosa* is associated with the host shift to mulberry. *Applied and Environmental*
570 *Microbiology* **80**, 3025-3033 (2014).
- 571 25 Randall, J. J. *et al.* Genetic analysis of a novel *Xylella fastidiosa* subspecies found in
572 the southwestern United States. *Applied and Environmental Microbiology* **75**,
573 5631-5638 (2009).
- 574 26 Nunney, L. *et al.* Recent evolutionary radiation and host plant specialization in
575 the *Xylella fastidiosa* subspecies native to the United States. *Applied and*
576 *Environmental Microbiology* **79**, 2189-2200 (2013).
- 577 27 Denancé, N. *et al.* Several subspecies and sequence types are associated with the
578 emergence of *Xylella fastidiosa* in natural settings in France. *Plant Pathology* **66**,
579 1054-1064 (2017).
- 580 28 EPPO. Normes OEPP EPP0 Standards - PM 7/24 (2) *Xylella fastidiosa*. *EPPO*
581 *bulletin* **46**, 463-500 (2016).
- 582 29 Olmo, D. *et al.* First detection of *Xylella fastidiosa* on cherry (*Prunus avium*) and
583 *Polygala myrtifolia* plants, in Mallorca Island, Spain. *Plant Disease* (2017).
- 584 30 Amanifar, N., Taghavi, M., Izadpanah, K. & Babaei, G. Isolation and pathogenicity
585 of *Xylella fastidiosa* from grapevine and almond in Iran. *Phytopathologia*
586 *Mediterranea* **53**, 318 (2014).

- 587 31 Çağlar, B. *et al.* First report of almond leaf scorch in Turkey. *Journal of Plant*
588 *Pathology* **87** (2005).
- 589 32 Su, C. C. *et al.* Pierce's disease of grapevines in Taiwan: Isolation, cultivation and
590 pathogenicity of *Xylella fastidiosa*. *European Journal of Plant Pathology* **161**, 389-
591 396 (2013).
- 592 33 Wallingford, A. K., Myers, A. L. & Wolf, T. K. Expansion of the range of Pierce's
593 disease in Virginia. *Online. Plant Health Progress* doi:10.1094/PHP-2007-1004-01-
594 BR. (2007).
- 595 34 Purcell, A. Environmental therapy for Pierce's disease of grapevines. *Plant*
596 *Disease* **64**, 388-390 (1980).
- 597 35 Feil, H. & Purcell, A. H. Temperature-dependent growth and survival of *Xylella*
598 *fastidiosa* in vitro and in potted grapevines. *Plant Disease* **85**, 1230-1234 (2001).
- 599 36 Anas, O., Harrison, U. J., Brannen, P. M. & Sutton, T. B. Effect of warming winter
600 temperatures on the severity of Pierce's disease in the Appalachian Mountains
601 and Piedmont of the Southeastern United States. *Online. Plant Health Progress*
602 doi:10.1094/PHP-2008-0718-01-RS. **1**, 450-459 (2008).
- 603 37 Lieth, J., Meyer, M., Yeo, K.-H. & Kirkpatrick, B. Modeling cold curing of Pierce's
604 disease in *Vitis vinifera* 'Pinot Noir' and 'Cabernet sauvignon' grapevines in
605 California. *Phytopathology* **101**, 1492-1500 (2011).
- 606 38 Keller, R. P., Lodge, D. M. & Finnoff, D. C. Risk assessment for invasive species
607 produces net bioeconomic benefits. *Proceedings of the National Academy of*
608 *Sciences* **104**, 203-207 (2007).
- 609 39 Bosso, L., Febbraro, M., Cristinzio, G., Zoina, A. & Russo, D. Shedding light on the
610 effects of climate change on the potential distribution of *Xylella fastidiosa*.
611 *Biological Invasions* **18**, 1759-1768 (2016).
- 612 40 Hoddle, M. S. The potential adventive geographic range of glassy-winged
613 sharpshooter, *Homalodisca coagulata* and the grape pathogen *Xylella fastidiosa*:
614 implications for California and other grape growing regions of the world. *Crop*
615 *Protection* **23**, 691-699 (2004).
- 616 41 Broennimann, O. & Guisan, A. Predicting current and future biological invasions:
617 both native and invaded ranges matter. *Biology Letters* **4**, 585-589 (2008).
- 618 42 Kamas, J. *et al.* Pierce's disease overview and management guide: A resource for
619 grape growers in Texas and other Eastern U.S. growing regions. (Texas A&M
620 AgriLife Ext., College Station, Texas., 2012).
- 621 43 Smith, D., Dominiak-Olson, J. & Sharber, C. First report of Pierce's disease of grape
622 caused by *Xylella fastidiosa* in Oklahoma. *Plant Disease* **93**, 762-762 (2009).
- 623 44 Fick, S. E. & Hijmans, R. J. WorldClim 2: new 1 - km spatial resolution climate
624 surfaces for global land areas. *International Journal of Climatology* **37**, 4302-4315
625 (2017).
- 626 45 Watanabe, M. *et al.* Improved climate simulation by MIROC5: mean states,
627 variability, and climate sensitivity. *Journal of Climate* **23**, 6312-6335 (2010).
- 628 46 Flato, G. *et al.* in *Climate Change 2013: The Physical Science Basis. Contribution of*
629 *Working Group I to the Fifth Assessment Report of the Intergovernmental Panel on*
630 *Climate Change* (eds T.F. Stocker *et al.*) 741-866 (Cambridge University press,
631 2013).
- 632 47 Van Vuuren, D. P. *et al.* The representative concentration pathways: an overview.
633 *Climatic Change* **109**, 5-31 (2011).
- 634 48 Agresti, A. *Categorical Data Analysis*. Second edn, (Wiley, 2002).

- 635 49 R Core Team. R: A language and environment for statistical computing. R
636 Foundation for Statistical Computing, Vienna, Austria. URL [https://www.R-](https://www.R-project.org/)
637 [project.org/](https://www.R-project.org/). (2017).
- 638 50 Venables, W. N. & Ripley, B. D. *Modern Applied Statistics with S.*, (Springer, 2002).
- 639 51 Christensen, R. H. B. ordinal - Regression Models for Ordinal Data. R package
640 version 2015.6-28. <http://www.cran.r-project.org/package=ordinal/>. (2015).
- 641 52 Franklin, J. *Mapping species distributions: spatial inference and prediction.*
642 (Cambridge University Press, 2010).
- 643 53 Busby, J. R. BIOCLIM: a bioclimate analysis and prediction system. *Plant Prot Q* **6**,
644 8-9 (1991).
- 645 54 Booth, T. H., Nix, H. A., Busby, J. R. & Hutchinson, M. F. BIOCLIM: the first species
646 distribution modelling package, its early applications and relevance to most
647 current MAXENT studies. *Biodiversity and Conservation* **20**, 1-9 (2014).
- 648 55 Carpenter, G., Gillison, A. & Winter, J. DOMAIN: a flexible modelling procedure for
649 mapping potential distributions of plants and animals. *Biodiversity and*
650 *Conservation* **2**, 667-680 (1993).
- 651 56 Lobo, J. M. The use of occurrence data to predict the effects of climate change on
652 insects. *Current Opinion in Insect Science* **17**, 62-68 (2016).
- 653 57 Phillips, S. J., Anderson, R. P. & Schapire, R. E. Maximum entropy modeling of
654 species geographic distributions. *Ecological modelling* **190**, 231--259 (2006).
- 655 58 Pearson, R. G., Raxworthy, C. J., Nakamura, M. & Townsend Peterson, A. Predicting
656 species distributions from small numbers of occurrence records: a test case using
657 cryptic geckos in Madagascar. *Journal of Biogeography* **34**, 102-117,
658 doi:10.1111/j.1365-2699.2006.01594.x (2007).
- 659 59 Hijmans, R. J., Phillips, S., Leathwick, J. & Elith, J. dismo: Species Distribution
660 Modeling. R package version 1.1-4. <https://CRAN.R-project.org/package=dismo>.
661 (2017).
- 662 60 Jiménez-Valverde, A. *et al.* Use of niche models in invasive species risk
663 assessments. *Biological Invasions* **13**, 2785-2797 (2011).
- 664 61 Daugherty, M. P., Zeilinger, A. R. & Almeida, R. P. P. Conflicting Effects of Climate
665 and Vector Behavior on the Spread of a Plant Pathogen. *Phytobiomes* **1**, 46-53
666 (2017).
- 667 62 Araújo, M. B. & New, M. Ensemble forecasting of species distributions. *Trends in*
668 *Ecology & Evolution* **22**, 42-47 (2007).
- 669 63 Marmion, M., Parviainen, M., Luoto, M., Heikkinen, R. K. & Thuiller, W. Evaluation
670 of consensus methods in predictive species distribution modelling. *Diversity and*
671 *Distributions* **15**, 59-69 (2009).
- 672 64 Elith, J., Kearney, M. & Phillips, S. The art of modelling range-shifting species.
673 *Methods in Ecology and Evolution* **1**, 330-342 (2010).
- 674 65 Purcell, A. Cold therapy of Pierce's disease of grapevines [Viral diseases, insect
675 vectors]. *Plant Disease Reporter* (1977).
- 676 66 Wickham, H. *ggplot2: Elegant Graphics for Data Analysis.* (Springer-Verlag, 2016).
- 677 67 Wilke, C. O. cowplot: Streamlined Plot Theme and Plot Annotations for 'ggplot2'.
678 R package version 0.7.0. <https://CRAN.R-project.org/package=cowplot>. (2016).
- 679 68 Yaseen, T. *et al.* On-site detection of *Xylella fastidiosa* in host plants and in “spy
680 insects” using the real-time loop-mediated isothermal amplification method.
681 *Phytopathologia Mediterranea* **54**, 488-496 (2015).

- 682 69 Cruaud, A. *et al.* Using insects to detect, monitor and predict the distribution of
683 *Xylella fastidiosa*: a case study in Corsica. *bioRxiv*,
684 doi:<http://dx.doi.org/10.1101/241513> (2018).
685 70 Cornara, D. *et al.* Transmission of *Xylella fastidiosa* by naturally infected *Philaenus*
686 *spumarius* (Hemiptera, Aphrophoridae) to different host plants. *Journal of Applied*
687 *Entomology* **141**, 80-87 (2016).
688 71 Saponari, M. *et al.* Infectivity and transmission of *Xylella fastidiosa* by *Philaenus*
689 *spumarius* (Hemiptera: Aphrophoridae) in Apulia, Italy. *Journal of Economic*
690 *Entomology* **107**, 1316-1319 (2014).
691 72 Goodwin, P. & Zhang, S. Distribution of *Xylella fastidiosa* in southern Ontario as
692 determined by the polymerase chain reaction. *Canadian Journal of Plant*
693 *Pathology* **19**, 13-18 (1997).
694 73 Milling, A., Meng, F., Denny, T. P. & Allen, C. Interactions with hosts at cool
695 temperatures, not cold tolerance, explain the unique epidemiology of *Ralstonia*
696 *solanacearum* race 3 biovar 2. *Phytopathology* **99**, 1127-1134 (2009).
697 74 Soberón, J. & Peterson, A. T. Interpretation of models of fundamental ecological
698 niches and species' distributional areas. *Biodiversity Informatics* **2**, 1-10 (2005).
699 75 Chauvel, G., Cruaud, A., Legendre, B., Germain, J.-F. & Rasplus, J.-Y. Rapport de
700 mission d'expertise sur *Xylella fastidiosa* en Corse., (French Ministry of
701 agriculture and food, Available at:
702 http://agriculture.gouv.fr/sites/minagri/files/20150908_rapport_mission_corse_xylella_31082015b.pdf, 2015).
703
704 76 Rasplus, J.-Y. *et al.* in *AFPP - 4e conférence sur l'entretien des jardins végétalisés et*
705 *infrastructures.* (Available from
706 http://arbestense.it/images/Annales_IJEVI_2016.compressed.pdf).
707

708 Acknowledgements

709
710 We thank Pauline De Jerphanion (ANSES) manager of the French national database of
711 *Xylella fastidiosa* in France as well as the DGAL and the SRAL or feeding that database.
712 We also thank Christian Lannou (INRA, SPE, France) for his interest and support during
713 the course of the project. This work was funded by grants from the SPE department of
714 the INRA (National Agronomic Institute). The funders had no role in study design, data
715 collection and analysis, decision to publish, or preparation of the manuscript. JPR thanks
716 the SNCF (French national railway company) whose recurrent delays allowed him to
717 deeply meditate on the results reported in here.

718 Figure and table captions

719
720
721 **Figure 1** (A) Pierce's disease (PD) severity map in the United States. Each locality is
722 associated to a PD severity index (low, moderate or high severity) on the basis of the
723 map available in Anas *et al.*³⁶ and Kamas *et al.*⁴². (B) Occurrence records for the ST6 and
724 ST7 strains in France. Occurrence records for (C) *Xylella fastidiosa* subsp. *pauca* and (D)
725 *Xylella fastidiosa* subsp. *multiplex* in the Americas.

726
727 **Figure 2** Predicted potential severity of Pierce's disease in Europe under current and
728 future climate conditions obtained from a cumulative link model (CLM). 1 = low severity,
729 2 = moderate severity, 3 = high severity. Current climate conditions are average
730 temperature for the period 1970-2000 extracted from the Worldclim database⁴⁴. Future

731 climate estimates were obtained from the MIROC5 global climate model (scenarios 4.5
732 and 8.5). A: Predicted PD severity index for the period 1970-2000. B: Predicted PD
733 severity index in 2050 with the scenarios RCP4.5. C: Predicted PD severity index in 2050
734 with the scenarios RCP8.5. Areas associated to climate conditions that are not met
735 within the range of conditions characterizing the set of reference points in the native
736 range (i.e. MESS index < 0 see material and methods) are shown in grey.

737

738 **Figure 3** Predicted potential distribution of *Xf* subsp. *pauca* in Europe under current and
739 future climate conditions obtained by fitting Bioclim and Domain models. Current
740 climate conditions are average temperatures for the period 1970-2000 extracted from
741 the Worldclim database. Future climate estimates were obtained from the MIROC5
742 global climate model (scenarios 4.5 and 8.5). A: Habitat suitability for the period 1970-
743 2000. B: Habitat suitability in 2050 for the scenario RCP4.5. C: Habitat suitability in 2050
744 for the scenario RCP8.5. D: Proportion of models predicting presence for the period
745 1970-2000. E: Proportion of models predicting presence in 2050 for the scenario
746 RCP4.5. F: Proportion of models predicting presence in 2050 for the scenario RCP8.5.
747 Maps A, B, C were obtained by averaging (ensemble forecasting) of the outputs of the
748 models Bioclim and Domain run with 3 different climate datasets (see details in Table
749 1). Maps D, E, F were obtained by averaging the presence/absence maps derived from
750 habitat suitability using the lowest presence threshold. Areas associated to climate
751 conditions that are not met within the range of conditions characterizing the set of
752 reference points in the native range (i.e. MESS index < 0 see material and methods) are
753 shown in grey.

754

755 **Figure 4** Predicted potential distribution of *Xf* subsp. *multiplex* in Europe under current
756 and future climate conditions obtained by fitting Bioclim and Domain models. Current
757 climate conditions are average temperatures for the period 1970-2000 extracted from
758 the Worldclim database. Future climate estimates were obtained from the MIROC5
759 global climate model (scenarios 4.5 and 8.5). A: Habitat suitability for the period 1970-
760 2000. B: Habitat suitability in 2050 for the scenario RCP4.5. C: Habitat suitability in 2050
761 for the scenario RCP8.5. D: Proportion of models predicting presence for the period
762 1970-2000. E: Proportion of models predicting presence in 2050 for the scenario
763 RCP4.5. F: Proportion of models predicting presence in 2050 for the scenario RCP8.5.
764 Maps A, B, C were obtained by averaging (ensemble forecasting) of the outputs of the
765 models Bioclim and Domain run with 3 different climate datasets (see details in Table
766 1). Maps D, E, F were obtained by averaging the presence/absence maps derived from
767 habitat suitability using the lowest presence threshold. Areas associated to climate
768 conditions that are not met within the range of conditions characterizing the set of
769 reference points in the native range (i.e. MESS index < 0 see material and methods) are
770 shown in grey.

771

772

773 **Figure 5** Predicted potential distribution of the French strains ST6 and ST7 (*Xf* subsp.
774 *multiplex*) in Europe under current and future climate conditions obtained by fitting
775 Bioclim and Domain models. Current climate conditions are average temperatures for
776 the period 1970-2000 extracted from the Worldclim database. Future climate estimates
777 were obtained from the MIROC5 global climate model (scenarios 4.5 and 8.5). A: Habitat
778 suitability for the period 1970-2000. B: Habitat suitability in 2050 for the scenario
779 RCP4.5. C: Habitat suitability in 2050 for the scenario RCP8.5. D: Proportion of models

780 predicting presence for the period 1970-2000. E: Proportion of models predicting
 781 presence in 2050 for the scenario RCP4.5. F: Proportion of models predicting presence
 782 in 2050 for the scenario RCP8.5. Maps A, B, C were obtained by averaging (ensemble
 783 forecasting) of the outputs of the models Bioclim and Domain run with 3 different
 784 climate datasets (see details in Table 1). Maps D, E, F were obtained by averaging the
 785 presence/absence maps derived from habitat suitability using the lowest presence
 786 threshold. Areas associated to climate conditions that are not met within the range of
 787 conditions characterizing the set of reference points in the native range (i.e. MESS index
 788 < 0 see material and methods) are shown in grey.
 789
 790

791 **Table 1.** Measures of Bioclim and Domain models transferability calculated for different
 792 climate datasets. The area under the curve of the receiver operator curve (AUC) and the
 793 sensitivity of each model were calculated on the basis of occurrence records available in
 794 the European invaded range for *Xf* subsp. *pauca* and *multiplex*. The climate datasets
 795 leading to the best performing models were #1, #4 and #7 for subsp. *pauca* and #2, #6
 796 and # 9 for subsp. *multiplex*. bio5: maximum temperature of the warmest month; bio6:
 797 minimum temperature of the coldest month; bio10: mean temperature of the warmest
 798 quarter; bio11: mean temperature of the coldest quarter.
 799

800 **Table 1.**

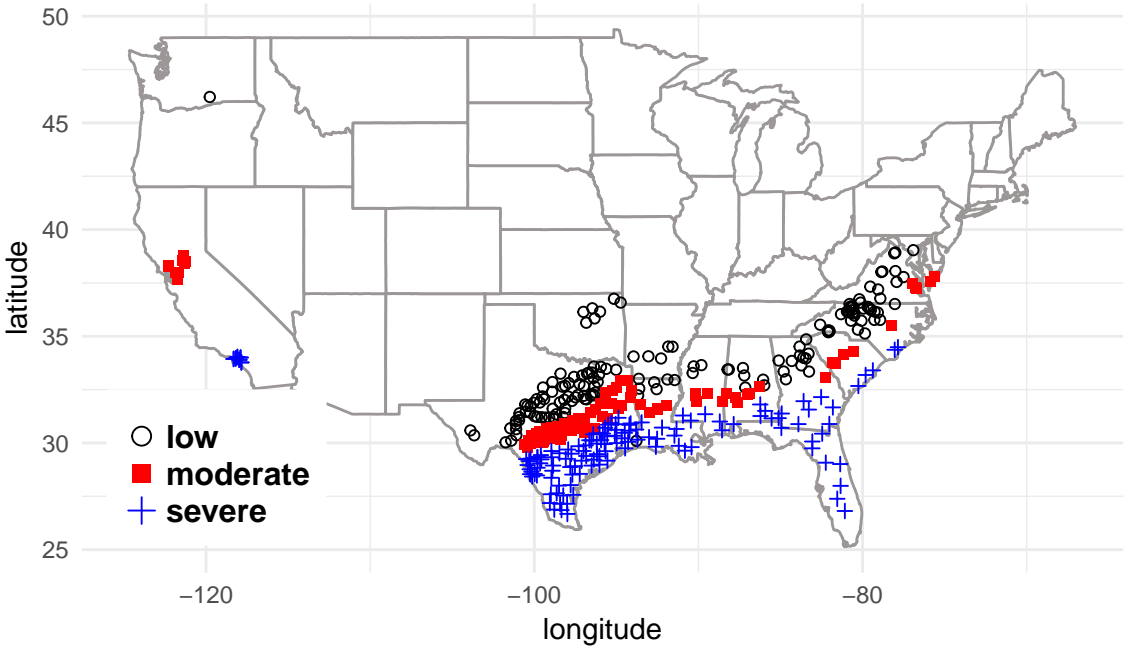
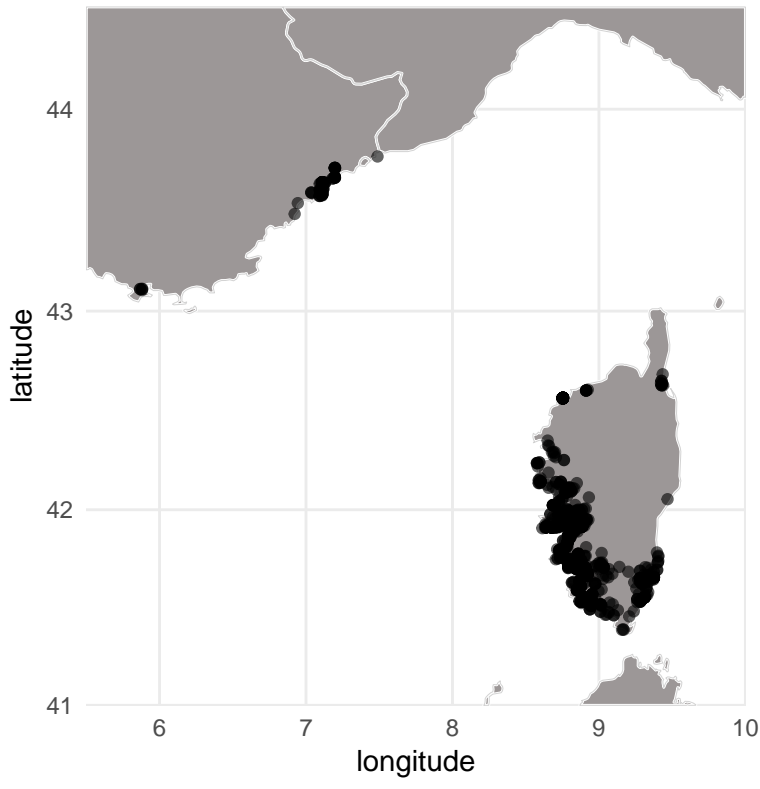
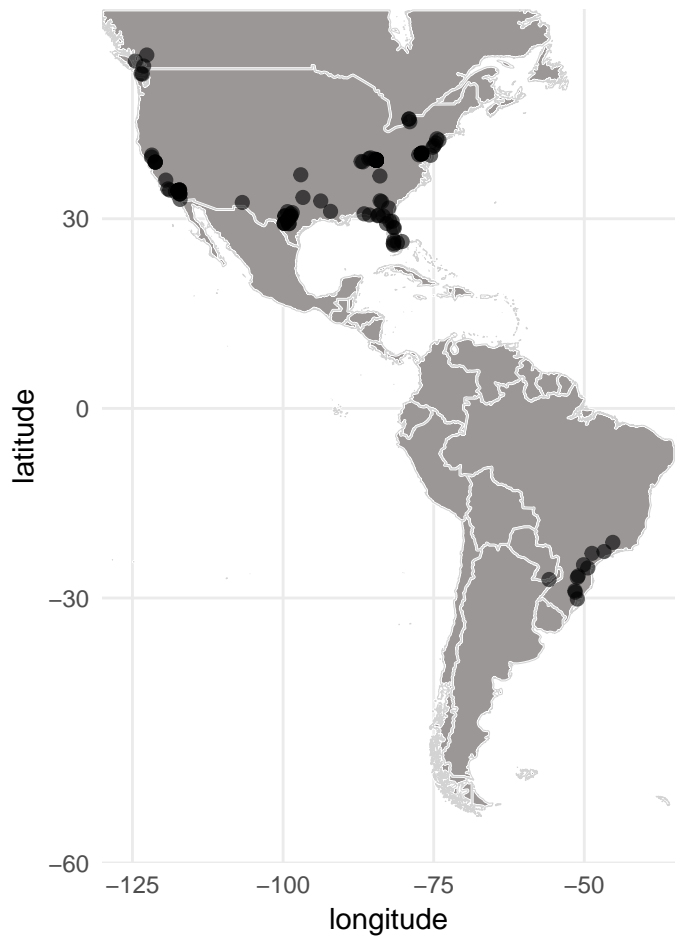
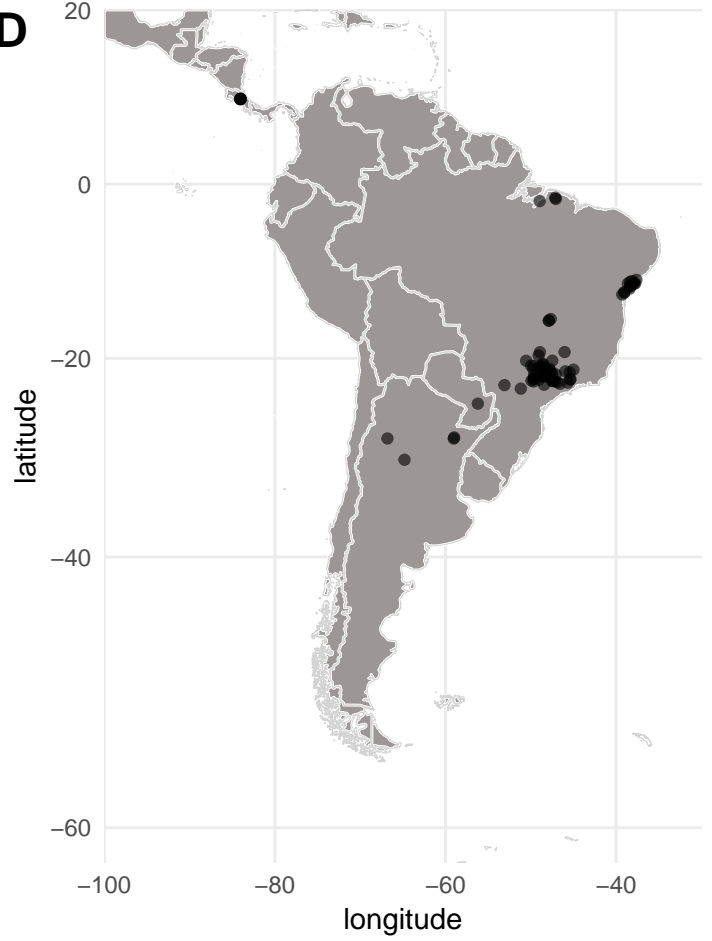
801

Dataset	Climate variables	Subspecies <i>pauca</i>				Subspecies <i>multiplex</i>			
		BIOCLIM		DOMAIN		BIOCLIM		DOMAIN	
		AUC	Sens.	AUC	Sens.	AUC	Sens.	AUC	Sens.
dataset #1	bio6	0.88	1	0.9	1	0.686	0.999	0.759	0.999
dataset #2	bio11	0.44	0.04	0.78	0.04	0.918	0.999	0.924	0.999
dataset #3	bio6, bio11	0.45	0.04	0.79	0.12	0.742	0.999	0.847	0.999
dataset #4	bio5, bio6	0.96	1	0.96	1	0.839	0.999	0.797	0.999
dataset #5	bio5, bio11	0.5	0.04	0.92	0.16	0.838	0.999	0.801	0.999
dataset #6	bio10, bio11	0.5	0.04	0.91	0.16	0.884	0.999	0.965	0.999
dataset #7	bio6, bio10	0.95	1	0.95	1	0.867	0.999	0.904	0.999
dataset #8	bio5, bio6, bio11	0.5	0.04	0.92	0.16	0.843	0.999	0.803	0.999
dataset #9	bio6, bio10, bio11	0.5	0.04	0.91	0.16	0.871	0.999	0.933	0.999
dataset #10	bio5, bio6, bio10, bio11	0.5	0.04	0.92	0.16	0.853	0.999	0.819	0.999

802

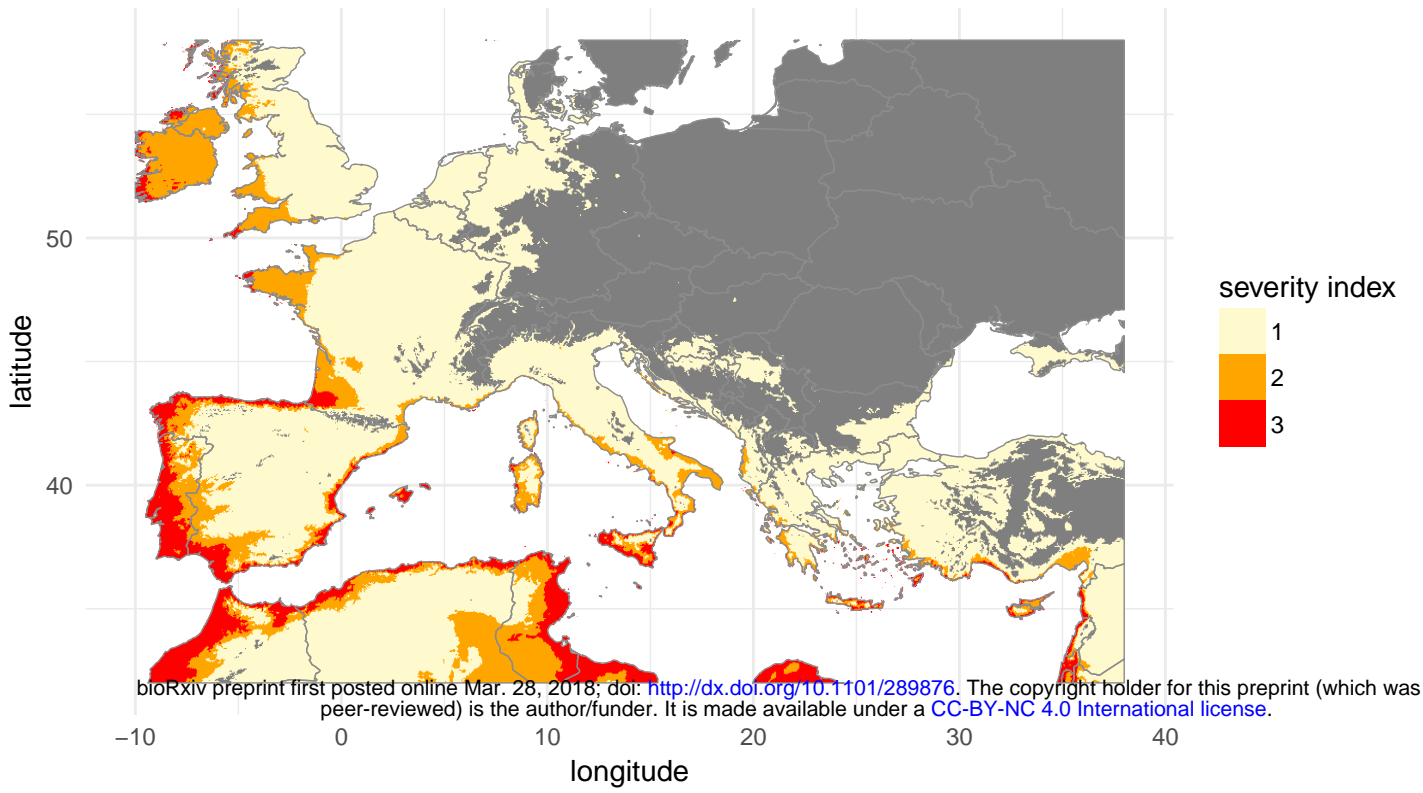
803

804 **Supplementary Information accompanies this paper and are available as a pdf file**
 805 (Godefroid_et al_Xylella_fastidiosa_Europe_suppl_mat.pdf)

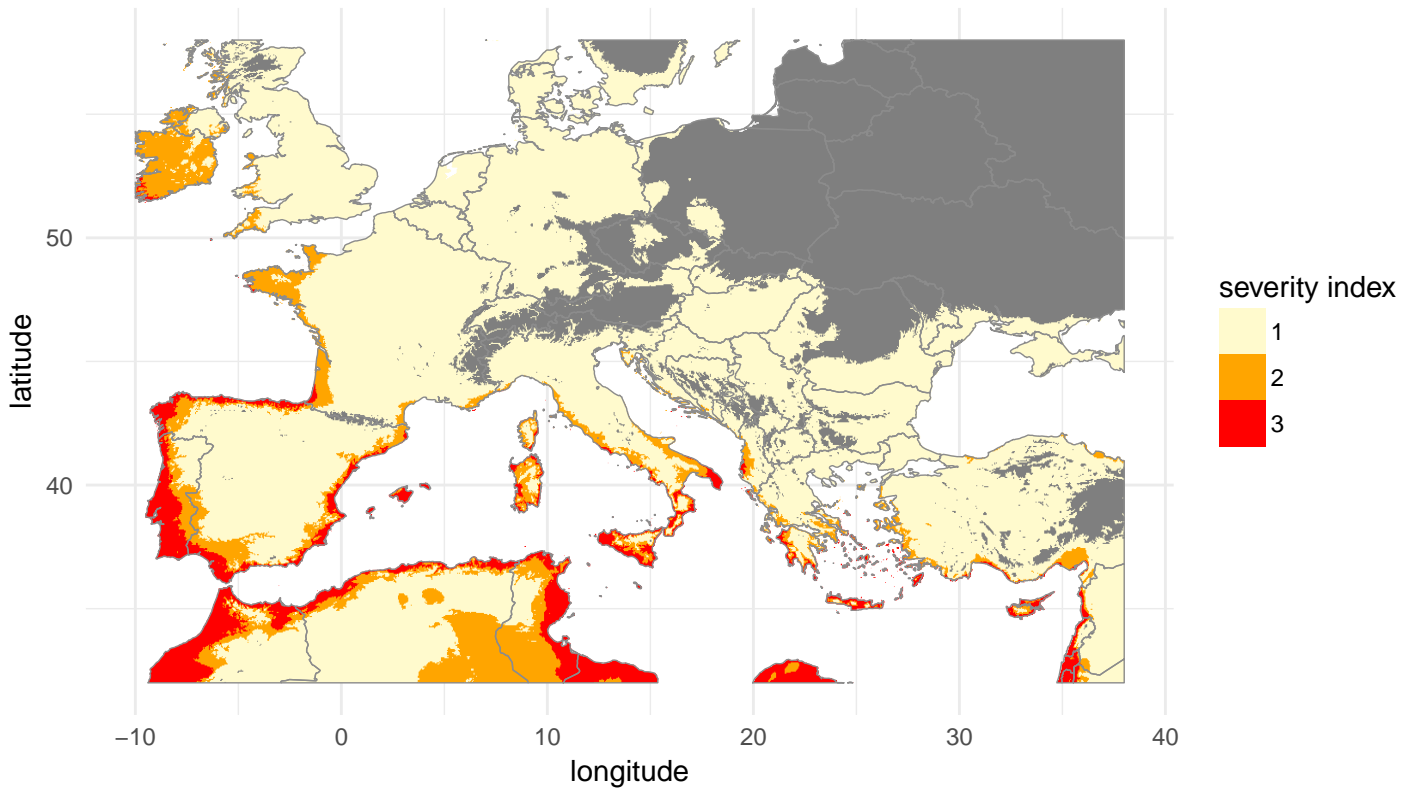
A**B****C****D**

A

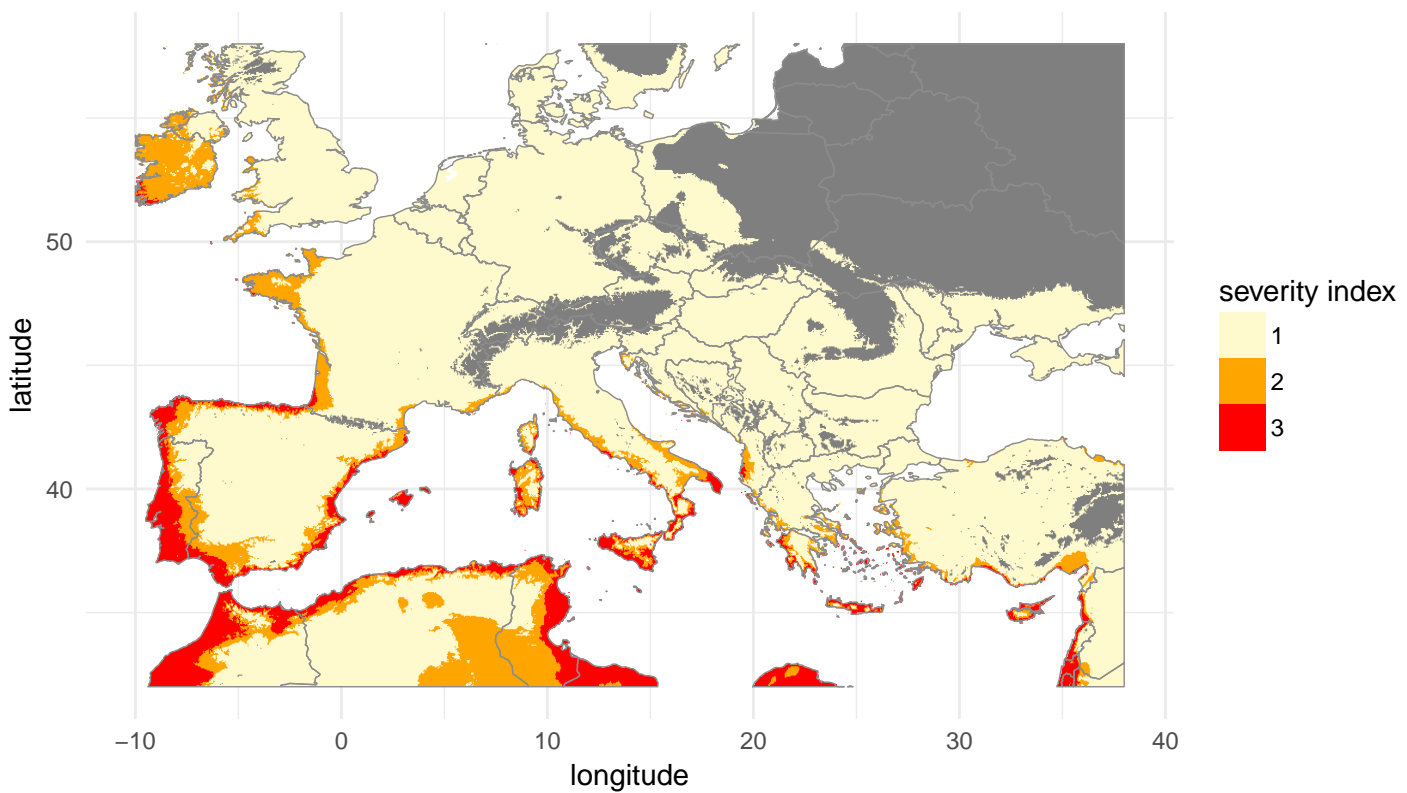
Pierce disease severity index 1970–2000

**B**

Pierce disease severity index 2050 [scenario 4.5]

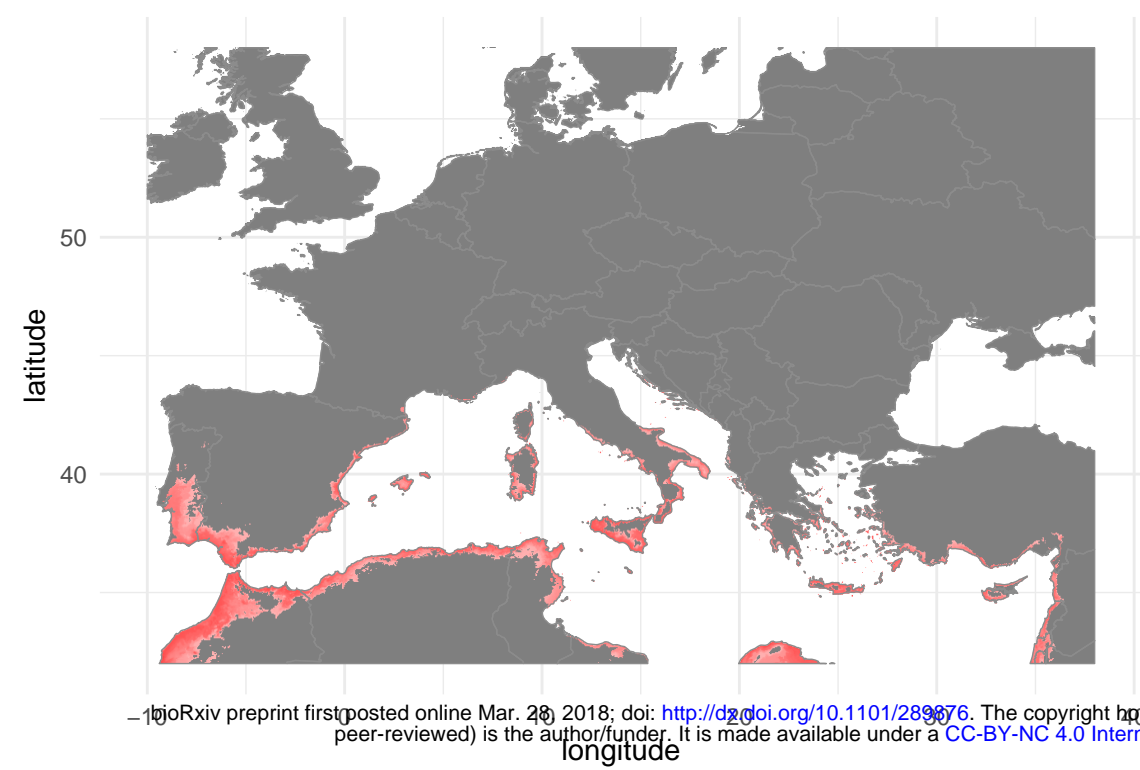
**C**

Pierce disease severity index 2050 [scenario 8.5]

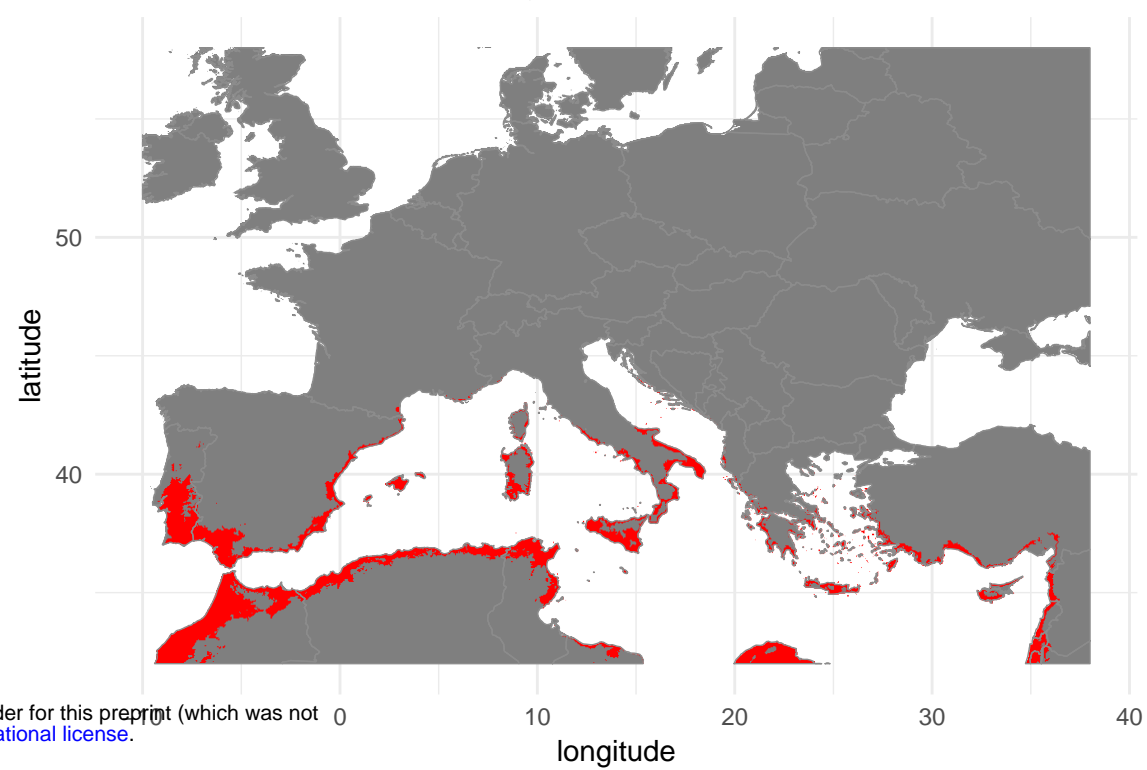


A

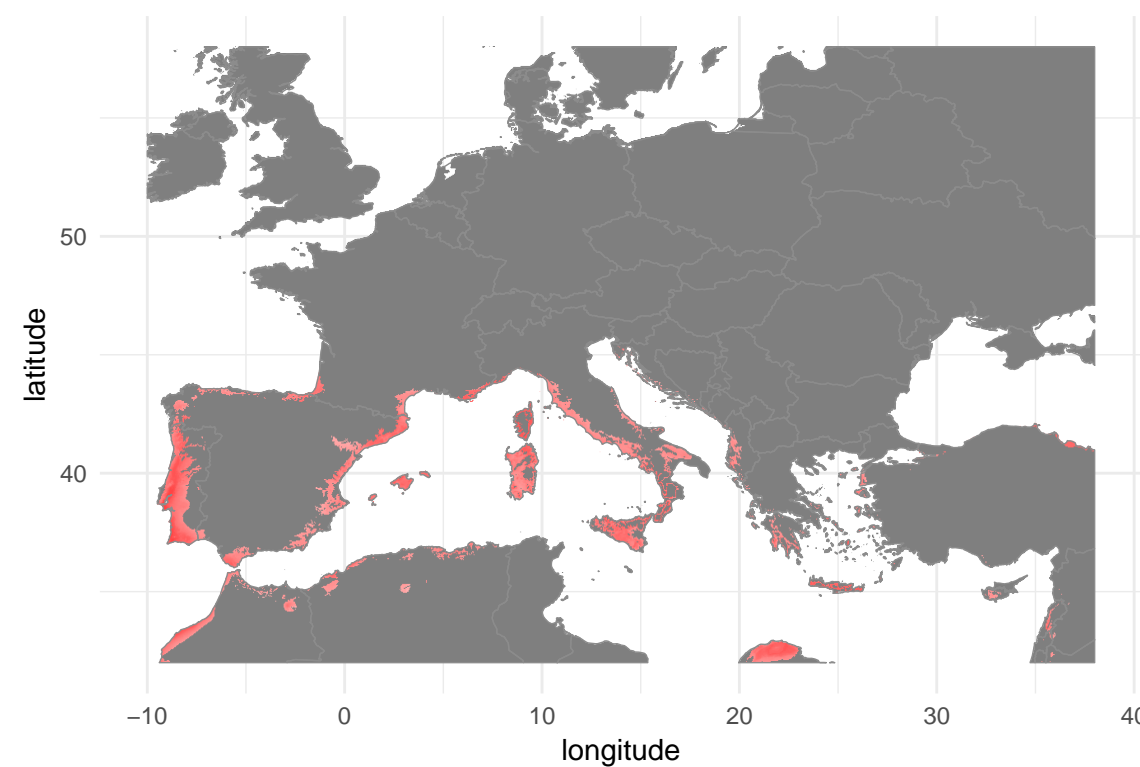
Habitat suitability 1970–2000

**D**

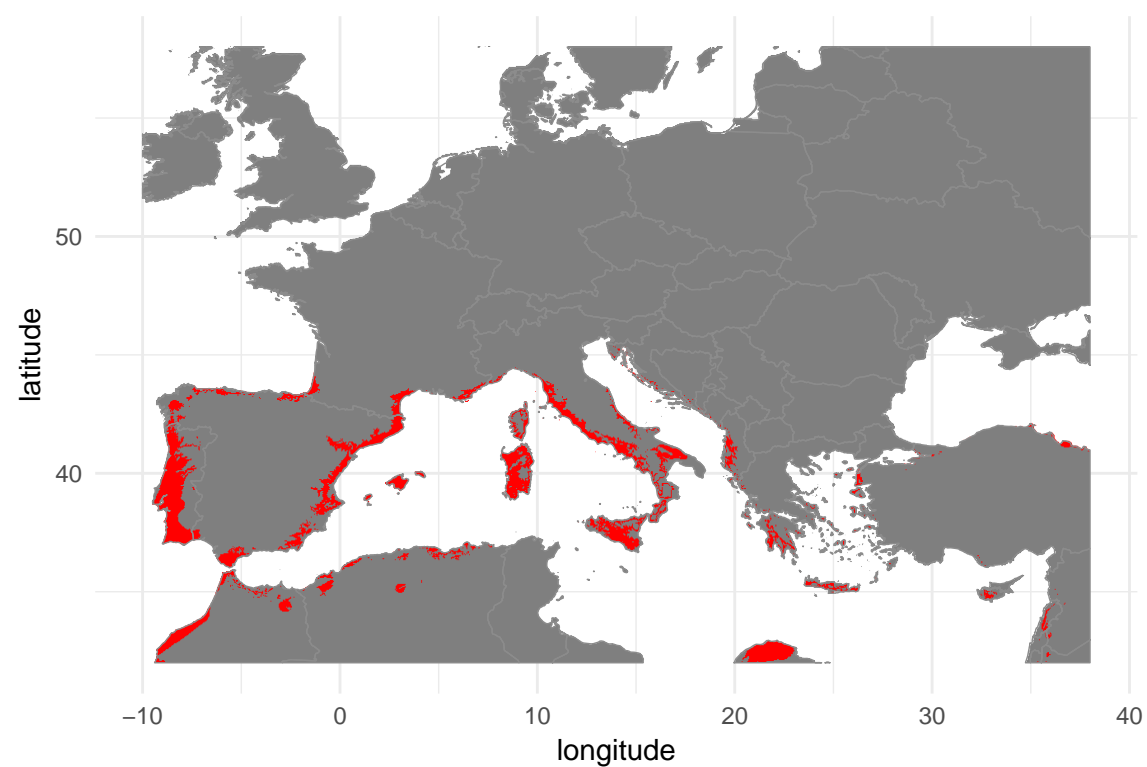
Proportion of models predicting presence 1970–2000

**B**

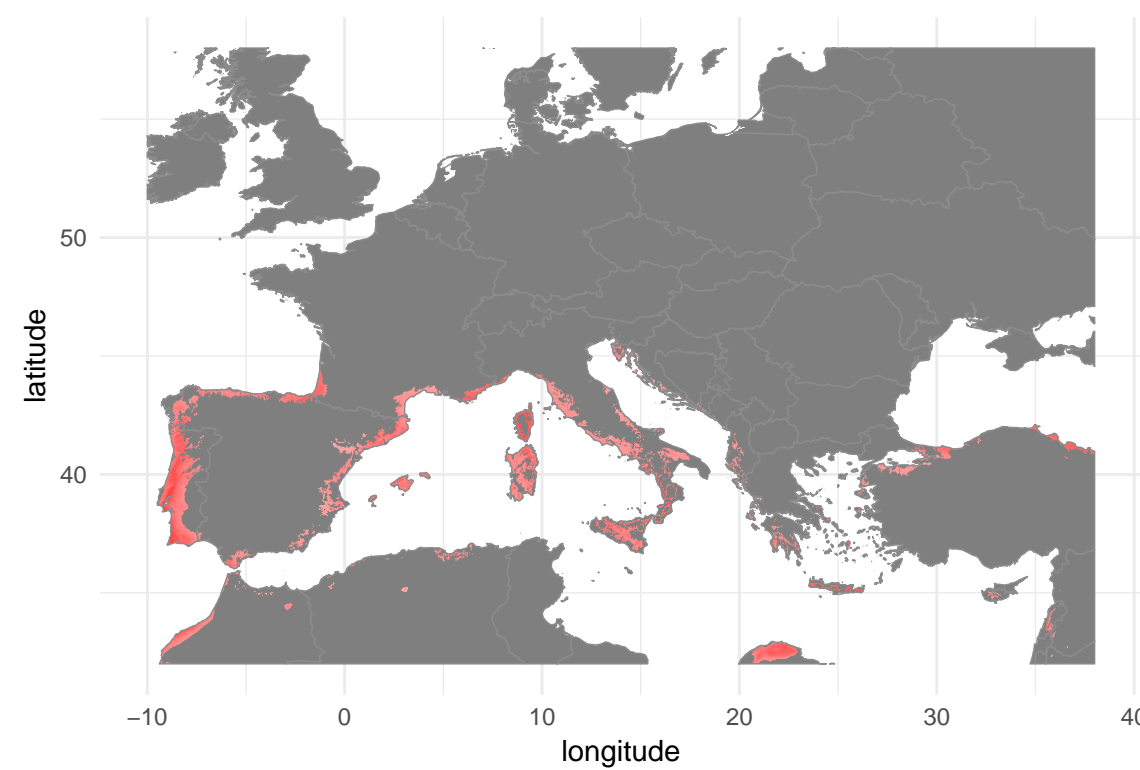
Habitat suitability 2050 [scenario 4.5]

**E**

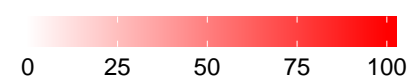
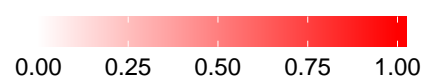
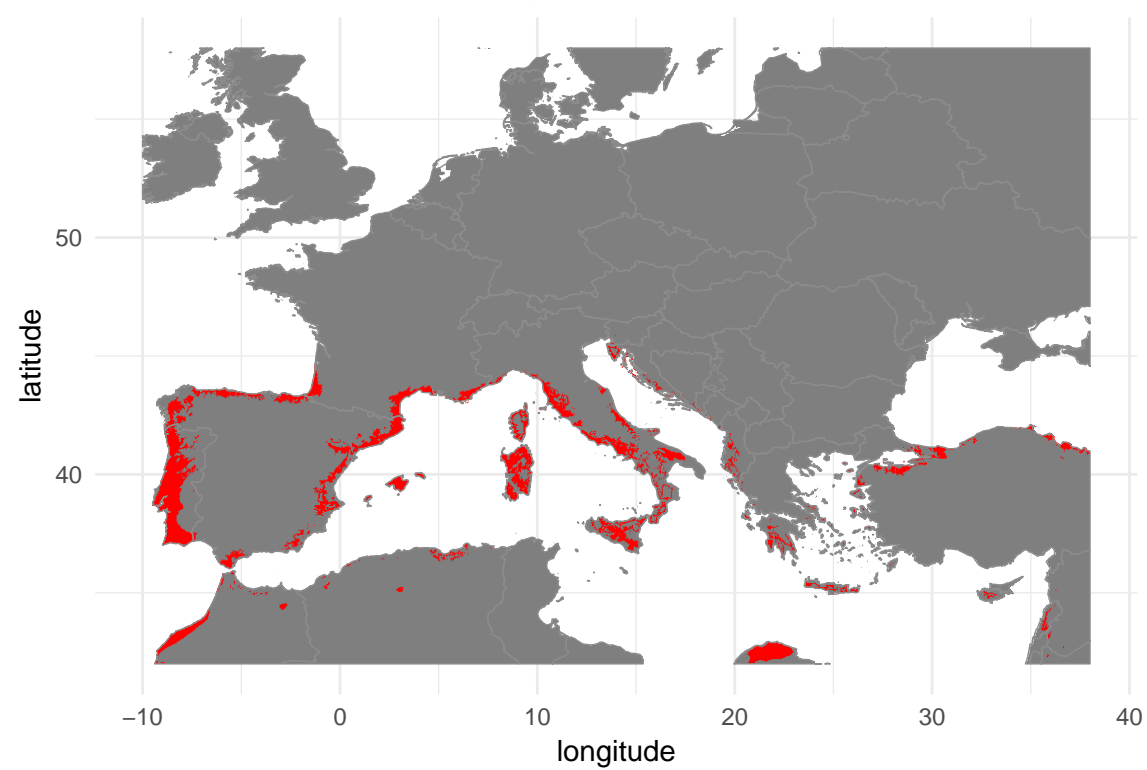
Proportion of models predicting presence 2050 [scenario 4.5]

**C**

Habitat suitability 2050 [scenario 8.5]

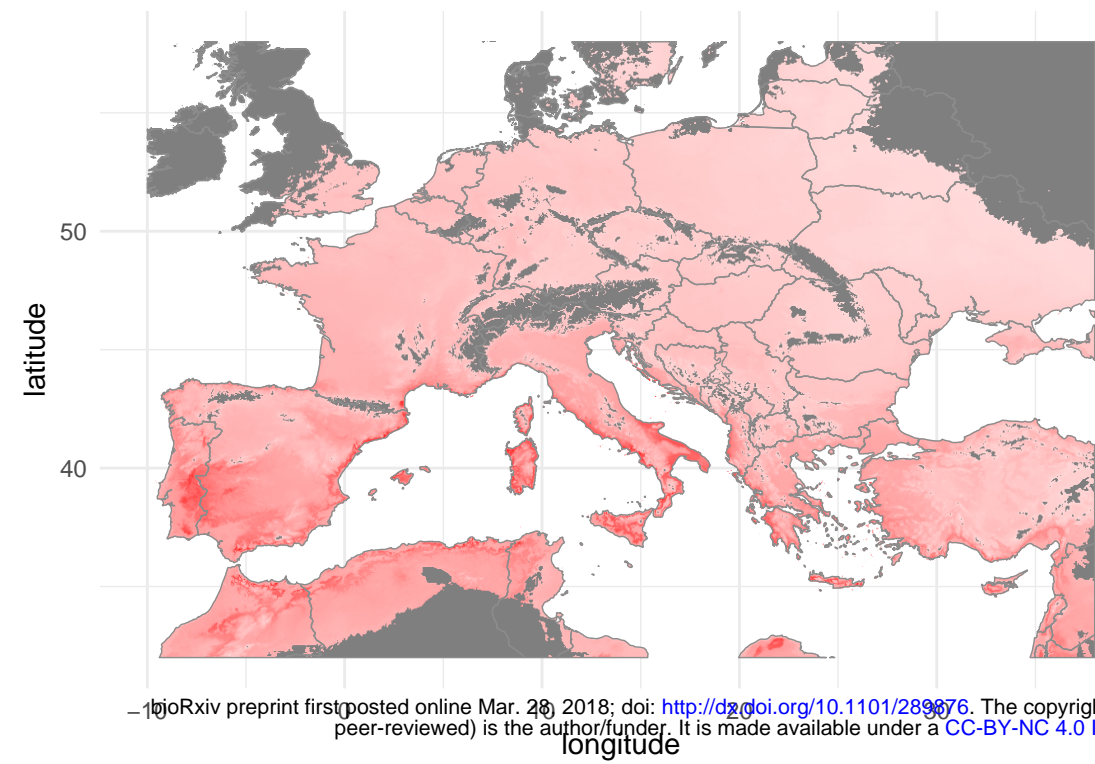
**F**

Proportion of models predicting presence 2050 [scenario 8.5]

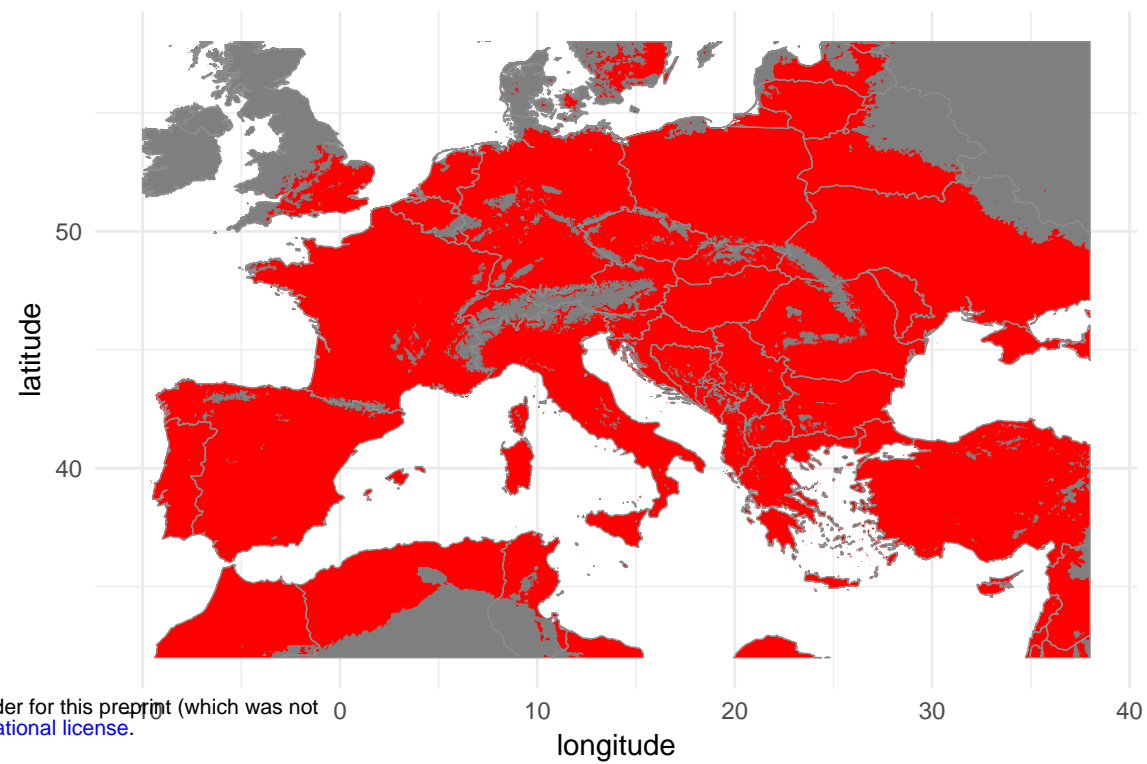


A

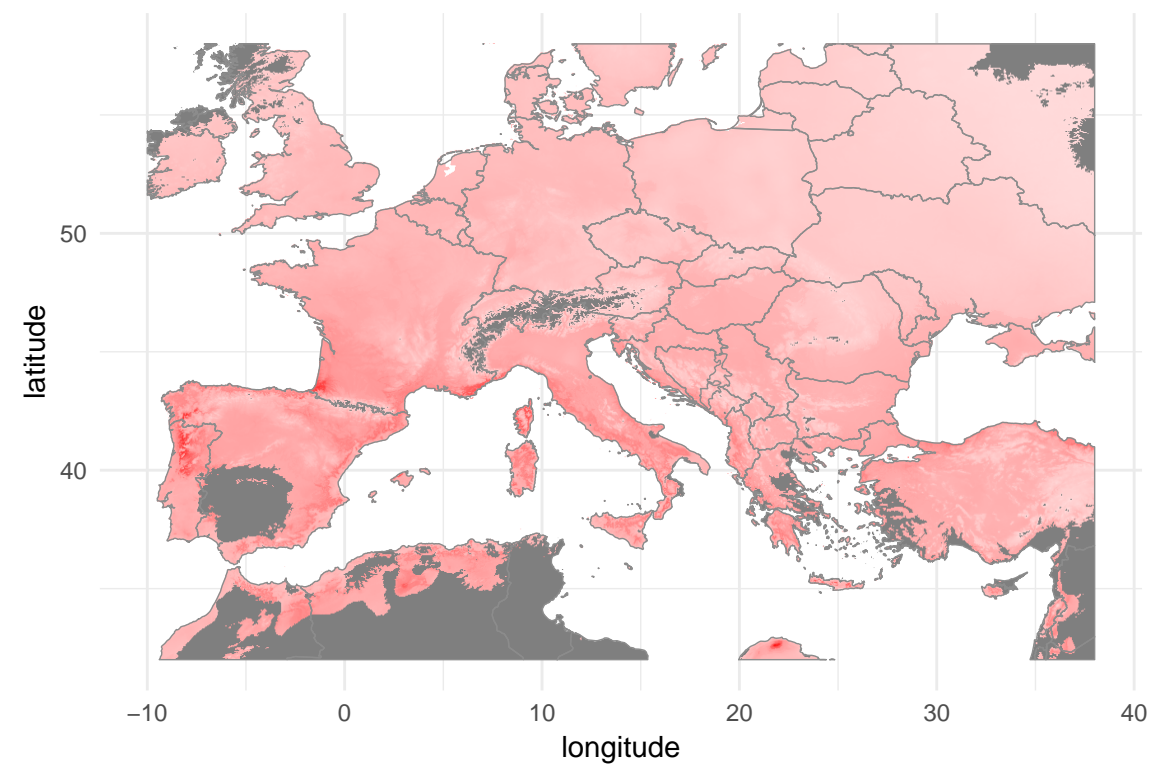
Habitat suitability 1970–2000

**D**

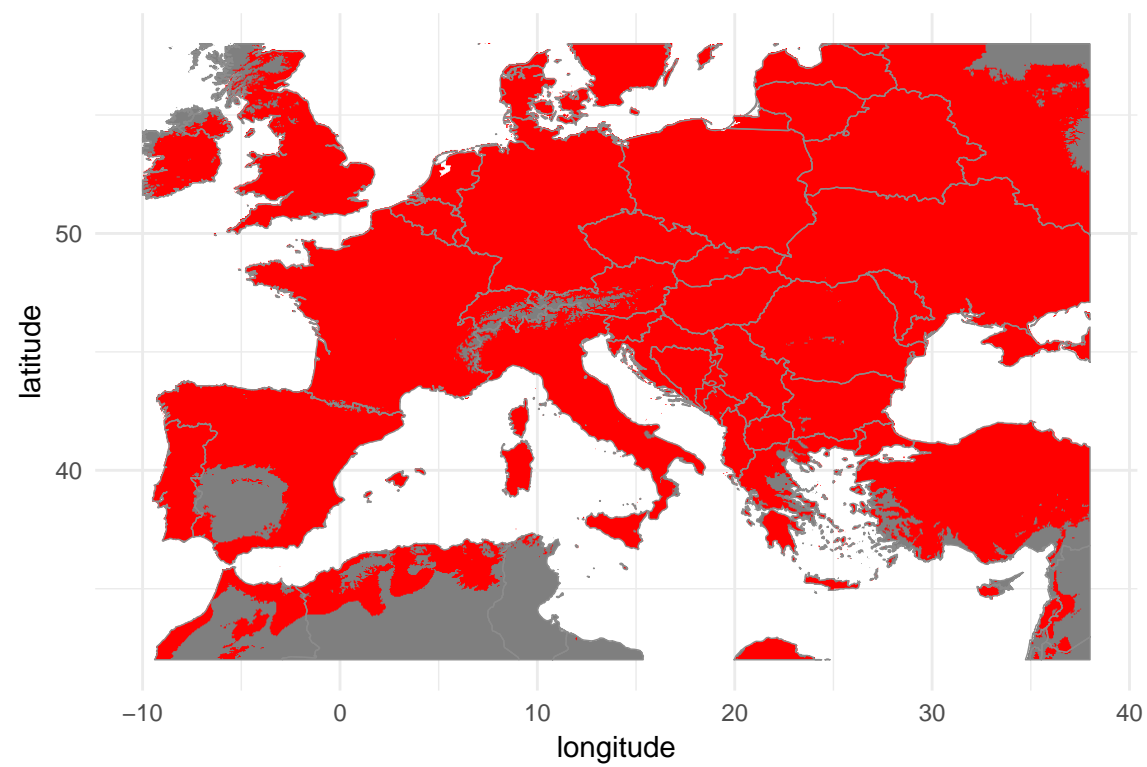
Proportion of models predicting presence 1970–2000

**B**

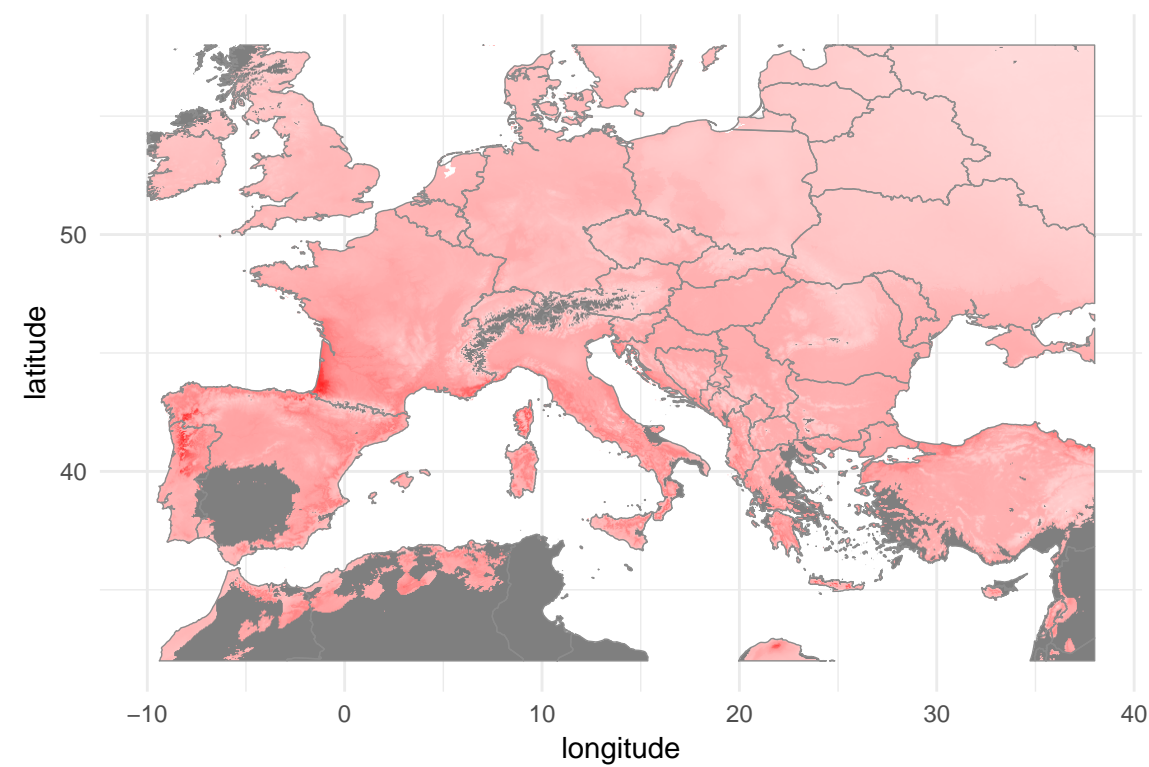
Habitat suitability 2050 [scenario 4.5]

**E**

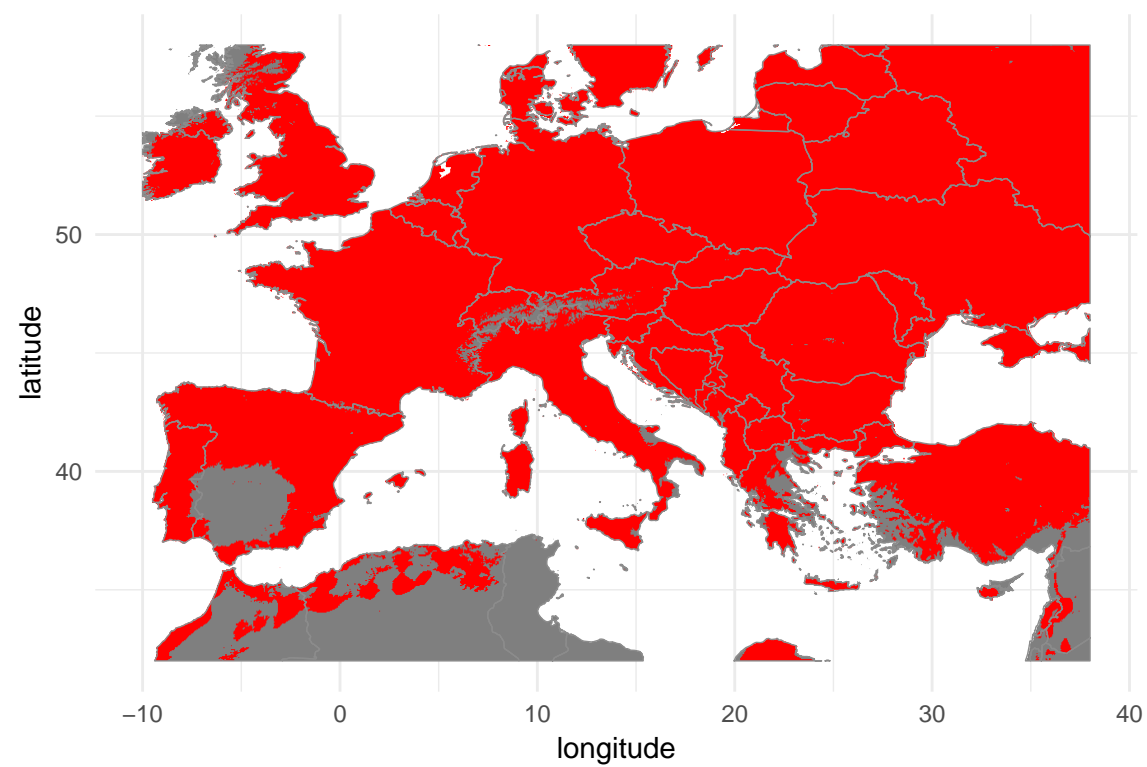
Proportion of models predicting presence 2050 [scenario 4.5]

**C**

Habitat suitability 2050 [scenario 8.5]

**F**

Proportion of models predicting presence 2050 [scenario 8.5]

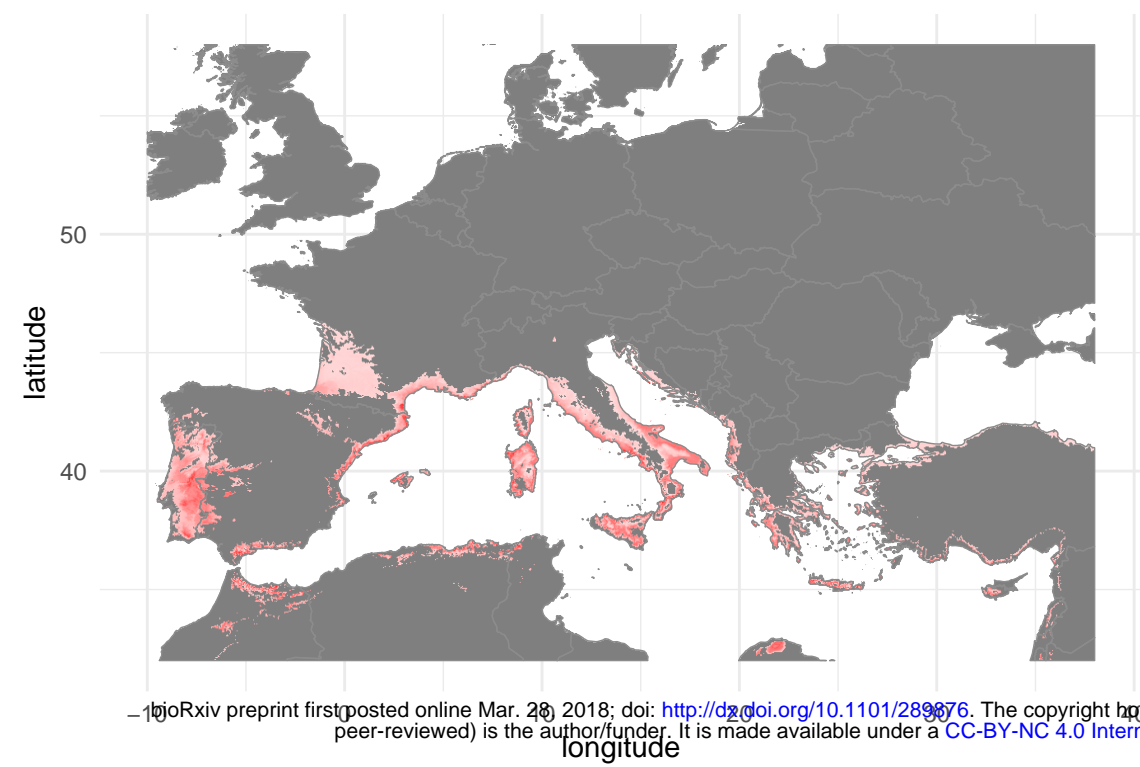


0.00 0.25 0.50 0.75 1.00

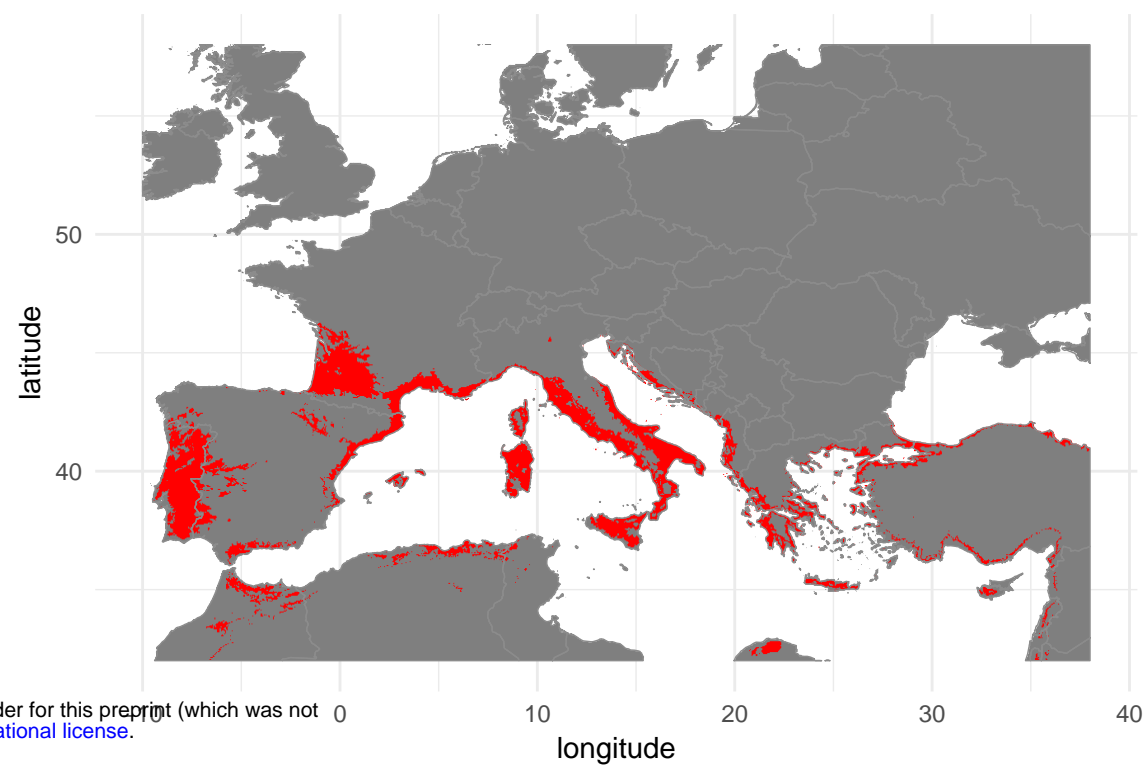
0 25 50 75 100

A

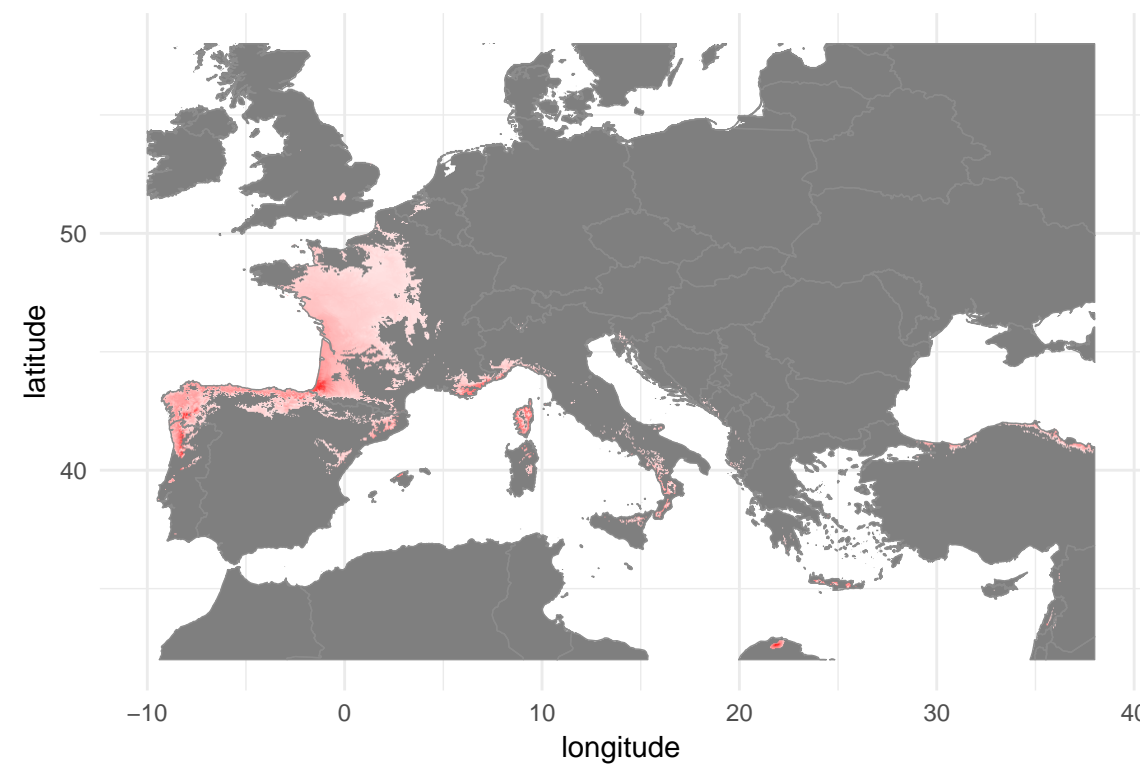
Habitat suitability 1970–2000

**D**

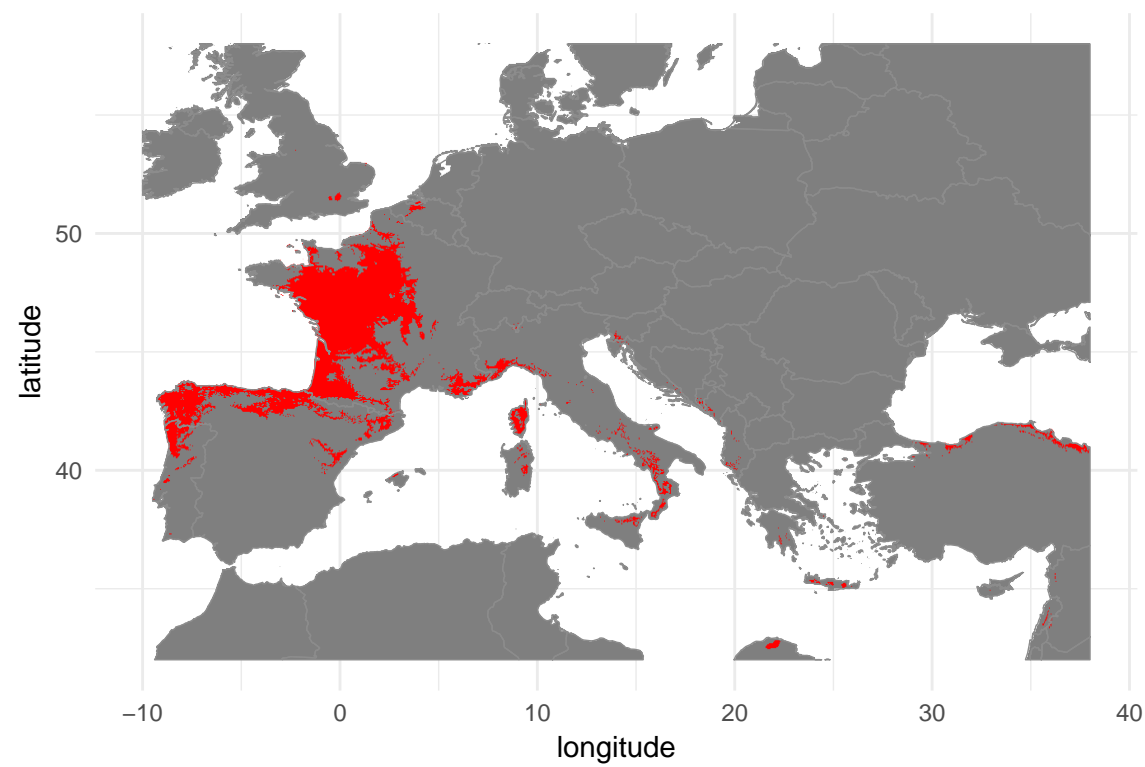
Proportion of models predicting presence 1970–2000

**B**

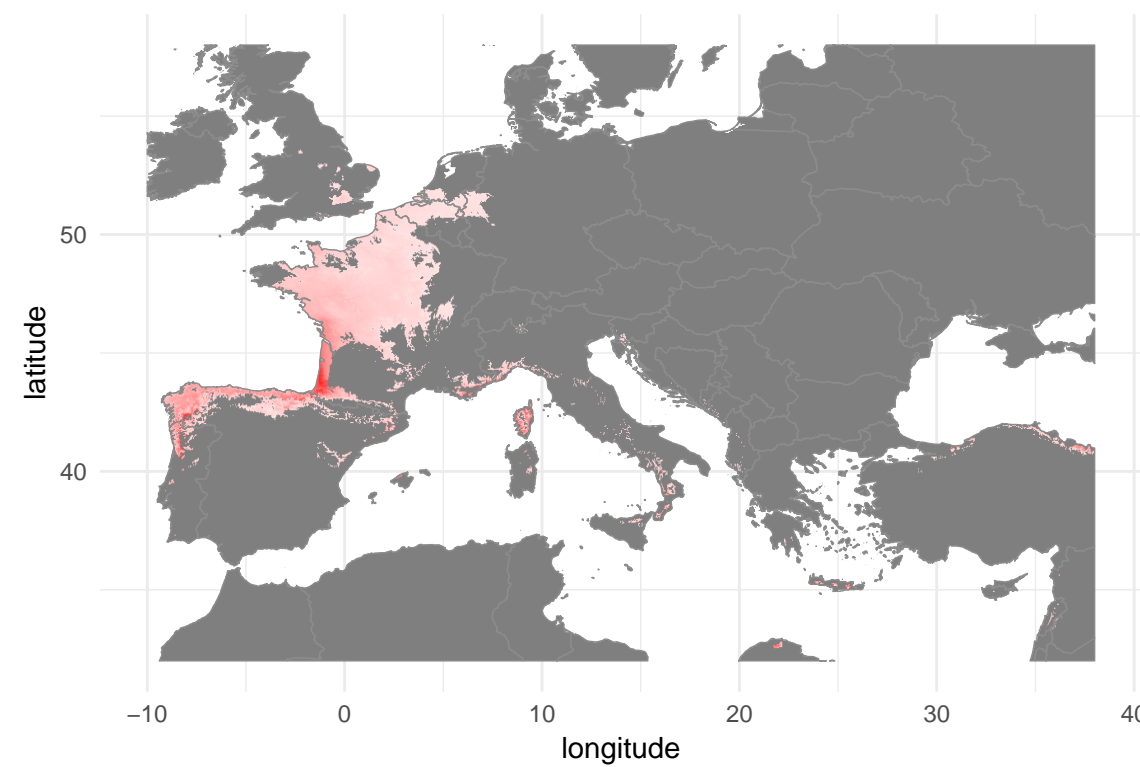
Habitat suitability 2050 [scenario 4.5]

**E**

Proportion of models predicting presence 2050 [scenario 4.5]

**C**

Habitat suitability 2050 [scenario 8.5]

**F**

Proportion of models predicting presence 2050 [scenario 8.5]

